HIF-1α accumulation in response to transient hypoglycemia may worsen diabetic eye disease

Chuanyu Guo[1,4], Monika Deshpande[1,4], Yueqi Niu[1], Isha Kachwala[1], Miguel Flores-Bellver[2], Haley Megarity[1], Taylor Nuse[1], Savalan Babapoor-Farrokhran[1], Michael Ramada[1], Jaron Sanchez[1], Neelay Inamdar[1], Thomas V. Johnson[1], Maria Valeria Canto-Soler[2], Silvia Montaner[3], Akrit Sodhi[1,5,*]

[1]Wilmer Eye Institute, Johns Hopkins University School of Medicine, Baltimore, MD 21287, USA

[2]*CellSight* Ocular Stem Cell and Regeneration Research Program, Department of Ophthalmology, Sue Anschutz-Rodgers Eye Center, University of Colorado School of Medicine, Aurora, CO 80045, USA

[3]Department of Oncology and Diagnostic Sciences, School of Dentistry, Greenebaum Cancer Center, University of Maryland, Baltimore, MD 21201, USA

[4]These authors contributed equally

[5]Lead contact

SUMMARY

Tight glycemic control (TGC), the cornerstone of diabetic management, reduces the incidence and progression of diabetic microvascular disease. However, TGC can also lead to transient episodes of hypoglycemia, which have been associated with adverse outcomes in patients with diabetes. Here, we demonstrate that low glucose levels result in hypoxia-inducible factor (HIF)-1-dependent expression of the glucose transporter, Glut1, in retinal cells. Enhanced nuclear accumulation of HIF-1α was independent of its canonical post-translational stabilization but instead dependent on stimulation of its translation and nuclear localization. In the presence of hypoxia, this physiologic response to low glucose resulted in a marked increase in the secretion of the HIF-dependent vasoactive mediators that promote diabetic retinopathy. Our results provide a molecular explanation for how early glucose control, as well as glycemic variability (i.e., oscillating serum glucose levels), contributes to diabetic eye disease. These observations have important implications for optimizing glucose management in patients with diabetes.

*Correspondence: asodhi1@jhmi.edu.

Graphical Abstract

In brief

Guo et al. show that transient episodes of hypoglycemia enhance the nuclear accumulation of HIF-1α, resulting in increased expression of GLUT1 in retinal glial cells. In the presence of hypoxia, this physiologic response results in a pathologic increase in the secretion of HIF-dependent angiogenic mediators that worsen diabetic eye disease.

INTRODUCTION

By 2050, the prevalence of diabetes will more than double globally, increasing the burden of this disease worldwide[1] and resulting in a concurrent increase in the number of patients with diabetic microvascular complications.[2] As therapies that help prevent the development or progression of diabetic retinopathy (DR), neuropathy, and nephropathy remain limited, strategies to minimize the impact of diabetic microvascular complications focus on optimizing glucose management.[3,4] Indeed, diabetic microvascular disease is strongly associated with the presence of chronic hyperglycemia, and results from multiple clinical trials consistently support a role for early and intensive glycemic control to reduce its onset and progression.[5] This has motivated clinicians to encourage their patients with diabetes to achieve tight glycemic control (TGC) to prevent or delay the development of the vascular complications that characterize this disease.

Unfortunately, TGC has also been associated with an early paradoxical worsening of DR,[6] the most common microvascular complication in patients with diabetes.[7] In the Diabetes Control and Complications Trial (DCCT), 13.1% of the treatment group using intensive insulin therapy had worsening of their DR compared with 7.6% of the treatment group using conventional insulin regimen. Although these effects were reversed in 18 months,[8] the cause of DR progression in this setting is not clear. Moreover, in patients in whom glycosylated hemoglobin (HbA1c) is safely lowered to target concentrations, the development of DR can be delayed, but not prevented. These results highlight the importance of pre-clinical studies examining how factors in addition to sustained elevation of serum glucose contribute to the development and progression of DR.[9]

Glycemic variability (transient episodes of very high, followed by very low glucose concentration) in patients with diabetes has also been implicated in the development or progression of micro- and macrovascular complications (and mortality) independent of HbA1c concentration.[10] For example, a patient with an HbA1c of 8.0% and high glycemic variability is at a higher risk of developing (or demonstrating progression of existing) DR than a patient with an HbA1c of 8.0% but who achieves low glycemic variability.[11] Based on this observation, it is speculated that retinal microvascular injury may result from even transient episodes of hyperglycemia.[12] Nonetheless, the molecular mechanism whereby brief changes in serum glucose concentration influences the development or progression of DR is not clear, and a contribution of hypoglycemia to DR is not known. Patients with insulin-dependent diabetes mellitus have an average of two symptomatic hypoglycemic episodes each week.[13] Patients with non-insulin-dependent diabetes mellitus also suffer from episodes of hypoglycemia, albeit less commonly, and most often while asleep.[14] Emerging evidence implicates recurrent subclinical (asymptomatic) hypoglycemic episodes in the promotion of cardiovascular disease[15] and cognitive decline.[16] In the current study, we set out to examine how the neurosensory retina responds to acute episodes of hypoglycemia, and how this response may contribute to the development and/or progression of diabetic eye disease.

RESULTS

Retinal cells cultured in low glucose (hypoglycemia) demonstrate a transient alteration in aerobic glycolysis

As glucose is the primary energy source for most cells and an important substrate for many biochemical reactions, transient episodes of hypoglycemia influence cell metabolism. The highly metabolically active neurosensory retina is particularly vulnerable to episodes of low glucose due to the strict dependence of retinal cells on glycolysis.[17] To interrogate the response of the retina to hypoglycemia, we isolated neurosensory retinal explants from 8- to 10-week-old mice and cultured them *in vitro* (Figure S1A). Hematoxylin and eosin staining of these retinal explants cultured for 24 h demonstrates preservation of the normal retinal architecture (Figure S1B) and the presence of the major inner retinal cell types (Figure S1C).

Using this retinal explant model, we explored the effect of acute hypoglycemia on retinal glycolysis by examining the $NAD^+/NADH$ in retinal explants cultured in low (2 mM, equal to approximately 36 mg/dL) D-glucose. While $NAD^+/NADH$ value is stable over time in

normal (5 mM, equal to approximately 90 mg/dL) D-glucose, it transiently increased at 2 h before gradually normalizing by 8 h in low glucose (Figure 1A). In mammalian retina, most pyruvate converted from glucose is reduced to lactate rather than metabolized in the tricarboxylic acid (TCA) cycle and oxidative phosphorylation, despite the availability of oxygen.[18,19] Under low glucose condition, the lactate level was decreased at 2 h when the NAD^+/NADH was elevated, but then also normalized by 8 h (Figure 1B). We postulated that this metabolic recovery of retinal cells following exposure to low glucose was mediated, in part, through the upregulation of glucose transporters. Accordingly, culturing retinal explants in low glucose resulted in an increase in mRNA expression of *Glut1*, but not *Glut3-5* (Figures 1C-1F); expression of *Glut2* mRNA was not detected by qPCR in the mouse neurosensory retina.

Müller glial cells are the principal storage site for glycogen and provide metabolic support to retinal neurons.[20,21] When the neurosensory retina is exposed to metabolic stress (e.g., hypoglycemia) the breakdown of glycogen in the Müller cells provides critical metabolites (e.g., lactic acid) for use by the deprived neurons, particularly in the inner nuclear and ganglion cell layers.[21] Retinal explants cultured in low glucose for 24 h demonstrated increased expression of glial fibrillary acidic protein (GFAP), an indicator of Müller cell stress (Figure 1G). This correlated with an increase in the expression of GLUT1 in Müller cells (Figure 1H). Expression of GLUT1 was similarly readily detected in an immortalized human Müller cell line (MIO-M1; Figure 1I) and increased with exposure to hypoglycemia (Figures 1J and 1K) for 16 h.

To characterize the expression of GLUT1 in human retinal cells in low glucose, we generated human induced pluripotent stem cell (hiPSC)-derived three-dimensional (3D) retinal organoids. By 120 days of differentiation (D120), the inner and outer retinal layers were clearly defined (Figures 1L and 1M) and contained the precursors of the major retinal cell types (Figure 1N). The increased GLUT1 expression observed in organoids cultured in low glucose colocalized with the Müller cell marker, CRALBP (Figure 1O).

Under hypoxic condition, *Glut1* is upregulated by the transcription factor, hypoxia-inducible factor (HIF)-1.[22] To examine whether the increase in mRNA expression of *Glut1* in the mouse neurosensory retina in response to low glucose was also dependent on HIF-1, we cultured retinal explant from adult mice that were heterozygous for HIF-1α.[23] Basal levels of HIF-1α are relatively normal in *Hif1a*^{+/−} mice, whereas in response to ischemia, HIF-1α expression is largely unchanged in *Hif1a*^{+/−} mice but potently stimulated in wild-type (*Hif1a*[wt]) littermate controls.[24] Increased *Glut1* mRNA in low glucose was attenuated in *Hif1a*^{+/−} compared with *Hif1a*[wt] mice (Figures 1P and 1Q). While the NAD^+/NADH was similarly increased in both *Hif1a*^{+/−} mice and their *Hif1a*[wt] littermates (Figure 1R), the decrease of NAD^+/NADH was diminished at 4 h in *Hif1a*^{+/−} mice (Figure 1R). Consistent with these results, we observed increased mRNA level of other HIF-regulated aerobic glycolysis genes in retinal explants cultured in low glucose (Figure S2).

Culturing retinal Müller cells in low D-glucose enhances accumulation of HIF-1α by promoting HIF-1α protein translation independent of its canonical post-translational modification

We next set out to interrogate the influence of low glucose on HIF-1α. MIO-M1 cells cultured in normoxia (20% O_2), and incrementally lower concentrations of glucose (from 5 to 0 mM) for 2 h, demonstrated expression of HIF-1α protein that was elevated in low glucose conditions and that peaked at approximately 2 mM glucose (Figure 2A). This was prior to any measurable change (reduction) in the glucose levels in the media (Figure S3). The increased accumulation of HIF-1α in low glucose was enhanced in cells cultured in hypoxia (1% O_2; Figure 2B). For this reason, subsequent studies interrogating the increase in HIF-1α accumulation in low glucose were performed in MIO-M1 cells cultured in 1% O_2. Interestingly, when we compared the expression of HIF-1α in MIO-M1 cells cultured in hypoxia (1% O_2) and hypoglycemia (0 or 2 mM), euglycemia (5 mM), or hyperglycemia (13, 25, or 50 mM; equal to approximately 234, 450, and 900 mg/dL, respectively), we only observed the increase in the accumulation of HIF-1α protein in cells cultured in low glucose (Figure 2C). These results were corroborated in primary retinal Müller cells isolated from the neurosensory retinas of postnatal day 3 (P3)–P5 C57BL/6J mice (Figure 2D) and in primary Müller cells isolated from both 3-day-old and 9-month-old immorto-mice[25] (Figures 2E, 2F, and S4A). We failed to observe an increase in HIF-1α protein accumulation in MIO-M1 cells cultured in low concentrations of the biologically inactive isomer L-glucose in media with 5 mM D-glucose (Figure S4B). Using L-glucose (Figure S4C) or mannitol (Figure S4D), we confirmed that the increase in HIF-1α protein accumulation in low D-glucose was not a consequence of low osmolarity.

To assess whether the dynamic reduction in glucose concentration (rather than the absolute concentration of glucose) promotes HIF-1α protein accumulation, we cultured MIO-M1 cells in high (25 mM) glucose for 1 week and then rapidly reduced the concentration of glucose from 25 mM to 20, 15, 10, 5, or 2 mM glucose and examined the levels of HIF-1α protein after 2-h exposure to the lower glucose concentration. We observed an increase in HIF-1α protein accumulation when the concentration of glucose was decreased from 25 mM to 0 and 2 mM, and also (albeit, to a lesser extent), when reduced to 5 or 10 mM, but not when the glucose concentration was decreased to 15 or 20mM (Figure 2G), suggesting that the dynamic reduction in glucose concentration (as occurs when patients with diabetes first undergo TGC) may also contribute to the accumulation of HIF-1α protein in MIO-M1 cells.

Canonical regulation of HIF-1α protein accumulation in response to hypoxia is mediated by post-translational modfications by the prolyl hydroxylase domain protein 2 (PHD2) and the ubiquitin ligase, von Hippel-Lindau protein (pVHL).[26] We there-fore examined whether inhibition of PHD2 (thereby inhibiting the PHD2/VHL system) with the prolyl hydroxylase inhibitor DMOG prevented the enhanced increase in HIF-1α accumulation observed in MIO-M1 cells cultured in low glucose. The accumulation of HIF-1α remained higher in MIO-M1 cells cultured in 2 mM glucose compared with cells cultured in 5 mM glucose despite treatment with DMOG (Figure 2H), suggesting that the increase in HIF-1α accumulation in low glucose was independent of its canonical regulation by the PHD2/VHL system. Indeed, MIO-M1 cells cultured in low glucose did not affect the mRNA or protein

levels of either *PHD2* or *VHL* in response to low glucose (Figures S4E-S2H). The $t_{1/2}$ of HIF-1α following exposure to the protein translation inhibitor, cyclohexamide (CHX), in cells cultured in 2 mM glucose (22 ± 2.1 min) was not significantly different compared with $t_{1/2}$ of HIF-1α in cells cultured in 5 mM glucose (18 ± 1.5 min; Figure 2I). Accordingly, prevention of the proteosomal degradation of HIF-1α with the proteasome inhibitor MG132 did not prevent the increase in HIF-1α accumulation observed in low glucose (Figure 2J). These results collectively demonstrate that increased accumulation of HIF-1α in low glucose does not require hypoxia, prolyl-hydroxylases, or the ubiquitin/proteasome degradation system.

We therefore shifted our focus upstream from HIF-1α protein stability. We first examined *HIF1a* mRNA transcription. We did not observe a significant change in the mRNA levels of *HIF1a* in MIO-M1 cells cultured in 2 mM compared with 5 mM glucose in normoxia or hypoxia (Figure 2K). We next examined HIF-1α translation. Since HIF-1α has a short half-life in normoxia (<2 min), for these studies we cultured MIO-M1 cells in 5 mM glucose in normoxia (20% O_2) but in the presence of the protea-some inhibitor MG132 for 2 h to prevent HIF-1α degradation. We then treated cells with CHX for 30 min to inhibit new protein translation, prior to changing the media to either low (2 mM) or normal (5 mM) glucose (and MG132 and CHX) for an additional 2 h. Inhibition of protein synthesis (with CHX) prevented the enhanced accumulation of HIF-1α observed in low (2 mM) compared with normal (5 mM) glucose (Figure 2L). These results suggest that the increase in HIF-1α protein accumulation in low glucose is independent of post-translational modification or mRNA transcription, but dependent on an increase in HIF-1α protein translation.

Nuclear accumulation of HIF-1α protein is enhanced in low glucose independent of protein translation

We next examined whether low glucose influences HIF-1α nuclear localization. Examination of the nuclear and cytoplasmic fractions of MIO-M1 cells exposed to hypoxia demonstrated an increase in nuclear accumulation of HIF-1α protein in cells cultured in 2 mM compared with 5 mM glucose (Figure 3A). Notably, this increase was markedly higher than the increase in HIF-1α protein observed in the cytoplasm. The increase in nuclear accumulation of HIF-1α was also observed in individual Müller cells by immunofluorescence (Figure 3B). Quantitation of cytoplasmic versus nuclear HIF-1α by immunofluorescence (Figure 3C) further suggested that the marked increase in nuclear accumulation of HIF-1α protein may be independent of total HIF-1α protein (Figure 3D). Indeed, when we pre-treated MIO-M1 cells with the proteosome inhibitor, MG132, to promote HIF-1α protein accumulation in the presence of CHX, we still observed enhanced accumulation of HIF-1α protein in the nuclear but not cytoplasmic fractions (Figure 3E). These results were corroborated by immunofluorescence (Figures 3F and 3G). Similar results were obtained when we inhibited HIF-1α protein degradation with MG132, blocked HIF-1α translation using CHX, and prevented hydroxylation of HIF-1α using the prolyl hydroxylase inhibitor DMOG (Figures 3H-3J). These observations collectively suggest that increased nuclear accumulation of HIF-1α in low glucose may occur by two independent mechanisms: an increase in protein translation and an increase in nuclear localization.

Accumulation of HIF-1α in mouse retinal explants and hiPSC-derived retinal organoids cultured in low glucose

We next examined the expression of HIF-1α protein in inner retinal cells in retinal explants cultured in low glucose. We observed an increase in expression of HIF-1α in retinal explants cultured in normoxia (20% O_2) as early as 1 h after exposure to low (2 mM) glucose (Figure 4A). This was prior to any measurable change (reduction) in the glucose levels in the media (Figure S5). Similarly, we observed a marked increase in the expression of HIF-1α in the inner nuclear layer of retinal explants cultured in 2 mM glucose for 4 h compared with 5 mM glucose by immunofluorescence (Figure 4B).

We have recently reported that hiPSC-derived 3D retinal organoids cultured in hypoxia (1% O_2) reproduce the increase in nuclear accumulation of HIF-1α protein observed in patients with ischemic retinopathies.[27] Retinal organoids are routinely cultured in high glucose (17.5 mM) and do not exhibit expression of HIF-1α protein when cultured in normoxia.[27] Lowering the glucose concentration from 17.5 mM to 2 mM glucose resulted in a marked increase in the expression of HIF-1α in normoxia throughout the retinal organoid (Figure 4C).

Low glucose enhances the angiogenic phenotype of retinal Müller cells

Hypoxic Müller cells have previously been reported to play a central role in promoting the angiogenic phenotype in patients with diabetic eye disease[28-32] as well as other ischemic retinopathies.[27,33,34] We therefore postulated that the increase in HIF-1α accumulation in Müller cells exposed to low glucose may enhance the angiogenic potential of these cells in conditions of hypoxia as occurs in patients with diabetic eye disease. Media conditioned by MIO-M1 cells cultured in hypoxia (i.e., 1% O_2) and 2 mM glucose demonstrated enhanced angiogenic potential (as determined by their promotion of endothelial cell tubule formation) compared with MIO-M1 cells cultured in hypoxia and 5 mM glucose (Figure 5A). These results were corroborated *in vivo* using the directed *in vivo* angiogenesis assay (DIVAA; Figure 5B).

Two HIF-regulated angiogenic mediators expressed by hypoxic retinal Müller cells, vascular endothelial growth factor (VEGF), and angiopoietin-like 4 (ANGPTL4) have previously been reported to participate in the progression of diabetic eye disease.[28,30-32] Culturing hypoxic MIO-M1 cells in 2 mM glucose resulted in a marked increase in *VEGF* and *ANGPTL4* mRNA expression compared with 5 mM glucose (Figures 5C and 5D). This increase correlated with an increase in VEGF and ANGPTL4 protein expression (Figures 5E and 5F). Increased mRNA expression of both *VEGF* and *ANGPTL4* in 2 mM glucose was also noted in cells cultured under normoxic conditions (Figures 5C and 5D, inset). The increased angiogenic potential of cells cultured in low glucose under normoxic conditions was confirmed *in vivo* using the DIVAA (Figure 5G).

While *Hifla*[wt] mouse embryonic fibroblasts (MEFs) also expressed increased levels of HIF-1α protein (Figure 5H) and *Vegf* and *Angptl4* mRNA (Figures 5I and 5J) when cultured in 2 mM glucose compared with 5 mM glucose, this was abolished in *Hif1a*^{−/−} MEFs.[35] These results were corroborated in cultured primary mouse retinal Müller cells from

Hif1a^flox/flox mice[36] infected with adenovirus expressing GFP (adeno-GFP) or expressing GFP and the Cre recombinase (adeno-GFP/Cre), the latter resulting in knockout of *Hif1a* (Figures 5K-5N). Collectively, these data demonstrate that low glucose enhances the expression of HIF-dependent vasoactive mediators, thereby promoting angiogenesis.

Activation of the Akt/mTOR signaling pathway in response to low glucose is not necessary for increased HIF-1α accumulation

To identify the signaling pathway that links low glucose to the increase in HIF-1α translation, we used a Phospho-Kinase Array Kit (Figure S6). We observed increased phosphorylation of multiple kinases in MIO-M1 cells cultured for 10 and 20 min in 2 mM compared with 5 mM glucose, several of which were down-stream of the Akt/mammalian target of rapamycin (mTOR) signaling pathway (Figures 6A and S6), previously implicated in the regulation of HIF-1α translation (Figure 6B).[37] Accordingly, MIO-M1 cells cultured in 2 mM glucose demonstrated an increase in phosphorylated (activated) Akt and mTOR compared with cells cultured in 5 mM glucose (Figure 6C). To determine whether mTOR activation contributed to the increase in HIF-regulated gene expression in low glucose, we used the pharmacologic mTORC1-specific inhibitor rapamycin; 1 μM rapamycin blunted the increase in *VEGF* and *ANGPTL4* mRNA expression (Figures 6D and 6E) and protein secretion (Figures 6F and 6G) in response to hypoxia in both 5 mM and 2 mM glucose. However, the relative increase in VEGF and ANGPTL4 mRNA and protein expression in cells cultured in 2 mM compared with 5 mM glucose was not affected by rapamycin. Similar results were observed with 1 mM of the dual mTORC1/2 inhibitor, AZD8055 (Figures 6H-6K). Collectively these results demonstrate that the Akt/mTOR pathway may be important for HIF-1α translation, but it is not necessary for the enhanced accumulation of HIF-1α observed in low glucose.

Hypoglycemia promotes HIF-dependent *Vegf* and *Angptl4* mRNA expression in mouse retina in the absence of hypoxia

We next cultured adult mouse retinal explants in low glucose and normoxia (20% O_2) and observed an increase in the mRNA expression of *Vegf* and *Angptl4* over time (Figures 7A and 7B). *Hif1a* mRNA expression was not affected (Figure 7C). The increased expression of *Vegf* and *Angptl4* mRNA in retinal explants cultured in low glucose was markedly reduced in *Hif1a^{+/−}* mice compared with their wild-type littermates (Figures 7D and 7E).

To corroborate these results, we injected intermediate-acting insulin (Novolin N) into mice to reproduce *in vivo* the transient episodes of hypoglycemia observed in patients with diabetes undergoing TGC (Figure 7F). In mice in which serum glucose levels were transiently (2–4 h) decreased to hypoglycemic levels (<40 mg/dL glucose), we observed increased HIF-1α protein accumulation in both the GCL and INL (Figure 7G). This correlated with an increase in *Angptl4* (but not *Vegf*) mRNA expression (Figures 7H and 7I); this increase was blunted by treatment of these animals with digoxin, which effectively inhibits the synthesis of HIF-1α protein.[38] Similar results were obtained in adult *Hif1a^{+/−}* mice compared with their *Hif1a^{wt}* littermates (Figures 7J and 7K). Collectively, these results demonstrate that low glucose, independent of hypoxia, can increase expression of HIF-1α and HIF-regulated vasoactive mediators that promote diabetic eye disease.

DISCUSSION

Balancing TGC with hypoglycemic episodes remains a challenge for patients with both insulin-dependent[13] and non-insulin-dependent[14] diabetes mellitus. Severe hypoglycemia can cause disorientation, loss of consciousness, and death. Moreover, recurrent subclinical (asymptomatic) hypoglycemic episodes have also been implicated in the promotion of cardiovascular disease[15] and cognitive decline.[16] These observations emphasize the importance of renewed efforts to better understand the impact of hypoglycemia on the morbidity and mortality of the growing diabetic population.

Although hypoglycemia has not been previously implicated in the development or progression of diabetic eye disease, it has been reported that high glycemic variability (significant oscillations in serum glucose) is a risk factor for DR independent of HbA1c.[11] It is assumed that brief episodes of increased serum glucose concentration (transient hyperglycemia) in patients with glycemic variability contribute to the development and progression of DR by promoting pericyte loss, endothelial cell injury, microaneurysms, and capillary dropout.[12] Damage to the retinal microvasculature, in turn, promotes retinal ischemia, the accumulation of the transcription factor HIF-1α, and increased expression of HIF-regulated vasoactive mediators.[39]

As glucose is the main metabolic and energy substrate for the retina,[18,40] the disruption of glucose metabolism may be expected to contribute to visual disease.[41] Here we demonstrate that low glucose transiently affects aerobic glycolysis and NAD^+ and lactate production in the vertebrate retina. One explanation for these observations is that low glucose promotes the switch from glycolysis to oxidative phosphorylation, thereby increasing oxygen consumption (and decreasing oxygen availability), resulting in the (hypoxic) accumulation of HIF-1α. However, retinal Müller cells obtain their ATP principally from glycolysis and have a remarkably low rate of oxygen consumption even in the presence of very low glucose for up to 4 h,[21] thereby sparing oxygen for resident retinal neurons. We demonstrate that retinal Müller cells respond to the reduced availability of glucose by increasing the HIF-dependent expression of the glucose transporter GLUT1. These results identify GLUT1 as a key regulator of Müller cell metabolism in conditions of low glucose.

We further report a previously unrecognized mechanism whereby hypoglycemia promotes increased HIF-1α translation and, independently, HIF-1α nuclear localization. Interestingly, the increase in HIF-1α translation in low glucose was not dependent on the Akt/mTOR pathway. This prompt physiologic regulatory mechanism to hypoglycemia ensures that retinal Müller cells are provided with a steady supply of glucose even under conditions when serum levels may be reduced. To further ensure steady energy, we observed that HIF-1 also increases expression of key glycolytic enzymes, including lactate by lactate dehydrogenase-A (LDHA) and pyruvate dehydrogenase kinase 1 (PDK1), the latter shunts pyruvate away from the TCA cycle. HIF-1α accumulation in hypoglycemia may thus play a key physiologic role in maintaining the health of retinal Müller cells.

However, we also demonstrate that this physiologic response to hypoglycemia may have a paradoxical pathological consequence. We report that the combination of increased

HIF-1α protein translation and its increased nuclear localization in hypo-glycemia results in a marked increase in the expression of HIF-regulated vasoactive gene products. In the setting of hypoxia, as occurs in patients with diabetic eye disease, this results in a synergistic increase in the expression of the HIF-regulated angiogenic gene products VEGF and ANGPTL4, both previously reported to play an important role in diabetic macular edema[30,32,42] and proliferative DR.[28,31] This, in turn, enhances the angiogenic phenotype of retinal Müller cells. These observations suggest that patients with underlying DR may be particularly vulnerable to transient decreases in glucose. While TGC remains essential for preventing microvascular injury in patients with diabetes, these findings suggest that this should not be achieved at the expense of glycemic stability. Collectively, these observations demonstrate that HIF-1 may be a particularly effective therapeutic target to prevent the development or progression of DR in patients with diabetes who struggle with high glycemic variability.

We also observed that in Müller cells chronically exposed to high glucose concentrations (as occurs in patients with undiagnosed or uncontrolled diabetes), a sudden reduction in glucose concentration to normal range (as occurs upon the initiation of therapies aimed at TGC) can also result in an increase in HIF-1α protein accumulation. This may help explain the observation in clinical trials demonstrating that TGC in patients with diabetes is associated with an early, paradoxical worsening of DR.[8] These results have important clinical implications for early optimization of serum glucose concentration in patients with diabetes and further suggest that HIF-1 may also be an important therapeutic target in patients with newly diagnosed diabetes.

Our results may also have implications for diabetic nephropathy[43] and diabetic neuropathy,[44] microvascular diseases in which hypoxia and HIF-1 also play an important role. Moreover, as acute glucose deprivation is a hallmark of other ischemic retinal diseases as well as ischemic disease affecting other tissue (e.g., myocardial infarction or stroke), our observations may have more broad implications that extend beyond patients with diabetes.

Conclusion

While TGC remains the most effective therapeutic option to prevent or delay the progression of diabetic eye disease, many patients who lower their HbA1c still go on to develop DR. We demonstrate here that the physiologic response of retinal cells to low serum glucose levels is to increase the nuclear accumulation of HIF-1α, and in turn, the expression of GLUT1, to ensure availability of this critical metabolite. However, in diabetic eye disease, this protective response may have a pathologic consequence. Accumulation of HIF-1α also leads to an increase in the expression of the angiogenic mediators that promote DR. These results have important clinical implications for optimizing glucose management in patients with diabetes.

Limitations of the study

An important limitation of the current study is the absence of correlative data in patients. Another limitation is that we were unable to identify the signaling pathway(s) connecting cellular detection of low glucose with the increase in nuclear accumulation of HIF-1α that

remains. These signaling cascades may ultimately provide new therapeutic targets for the treatment of DR.

STAR★METHODS

Detailed methods are provided in the online version of this paper and include the following:

RESOURCE AVAILABILITY

Lead contact—Further information and requests for resources and reagents should be directed to and will be fulfilled by the lead contact, Akrit Sodhi (asodhi1@jhmi.edu).

Materials availability—Commercially available reagents are listed in the key resources table. This study did not generate new unique reagents.

Data and code availability—The uncropped images of gels and immunoblots have been deposited to Mendeley Data and are publicly available as of the date of publication. The DOI is https://doi.org/10.17632/cx4zpmmwbx.1.

This paper does not report original code.

Any additional information required to reanalyze the data reported in this paper is available from the lead contact upon request.

EXPERIMENTAL MODEL AND SUBJECT DETAILS

Constructs and reagents—MG132 was obtained from Sigma (Sigma, Cat# M7449-1ML), Dimethyloxalylglycine (DMOG) from Cayman Pharmaceuticals (Cayman Pharmaceuticals, Cat# 71210), Digoxin from Sigma (Sigma, Cat# D6003-1G), Cycloheximide from Cell Signaling (Cell Signaling, Cat# 2112). pCEFL EGFP/Full Length HIF-1α plasmid was a generous gift from Gutkind (National Institute of Dental and Craniofacial Research, NIH, Bethesda, Maryland). D-glucose (Sigma, Cat# G5767) and L-glucose (Sigma, Cat# G5500) were purchased from Sigma. Hypoxia chambers (Coy Laboratory Products, Inc.) were used to expose cells or tissues to 1 or 3% oxygen.

Mice—All studies involving mice were approved by the Johns Hopkins University Animal Care and Use Committee and were performed in accordance with the NIH Guide for the Care and Use of Laboratory Animals. The mice were treated in accordance with the Association for Research in Vision and Ophthalmology Statement for the Use of Animals in Ophthalmic and Vision Research and the guidelines of the Johns Hopkins University Animal Care and Use Committee. C57BL/6J (Stock No, 000,664), immortomouse (Stock No, 032,619), $Hif1a^{+/-}$ mice (Stock No, 026,270), and HIF1$\alpha^{\text{flox/flox}}$ mice (Stock No, 007,561) were obtained from Jackson laboratory (Bar Harbor, ME). Eight-week-old nu/nu mice were obtained from Charles River Laboratories, Vermont, USA. Both male and female mice were used in all experiments in this study.

Cell culture—MIO-M1 cells were a generous gift from Astrid Limb (University College London Institute of Ophthalmology) and cultured with DMEM (Gibco, Cat# 11-885-092)

containing 1 g/L glucose with 10% FBS (Gibco, Cat# 16000044) and 1% penicillin/ streptomycin (Corning, Cat# 30-002-CI). Immortalized human dermal microvascular endothelial cells (HMEC1) were obtained from the CDC and cultured with high-glucose (4.5 g/L) DMEM (Corning, Cat# 10-013-CV) with 10% FBS (Gibco, Cat# 16000044) and 1% penicillin/streptomycin (Corning, Cat# 30-002-CI). *Hif1a^{wt}* and *Hif1a^{-/-}* MEFs were a generous gift from Gregg L. Semenza (Department of Pediatrics and Medicine, Johns Hopkins University School of medicine) and were cultured in 4.5 g/L glucose DMEM supplemented with 10% FBS, 0.1 mM nonessential amino acids, and 10 mg/mL bovine insulin. Primary Müller cells were isolated form C57BL/6J, immortomouse (a transgenic mouse line with inducible expression of a temperature-sensitive SV40 Large T Antigen enabling transient transformation of cells), or HIF1α^{flox/flox} mice and were cultured in high-glucose (4.5 g/L) DMEM (Corning, Cat# 10-013-CV) supplemented with 10% FBS (Gibco, Cat# 16000044) and 1% penicillin/streptomycin (Corning, Cat# 30-002-CI). The Müller cells from Hif1a^{flox/flox} were infected with either Ad5-CMV-eGFP or Ad5-CMV-Cre-eGFP (Adenovirus Vectors Service, Baylor College of medicine, Houston, TX). Before treatments, the growth media was replaced with serum starvation media containing 1% FBS (Gibco, Cat# 16000044).

METHOD DETAILS

Retinal explant isolation and culture—Retinal explant isolation was performed from mice euthanized with CO_2.[45] Followed by a circumferential incision made around the limbus of eyes enucleated from 8 to 10-week-old mice, the anterior segment, lens, and vitreous body were removed. The retina was peeled away from the choroid and was dissected radially into four equalized quadrants. After transferring the retinal explants onto 30-mm diameter filters (Millipore, Cat# PICM03050) with the RGC side facing up, the filters were placed into 6-well plate with 1.5 mL Neurobasal-A Medium (ThermoFisher, Cat# A2477501), supplemented with 2% B27 (Gibco, Cat# 17504044), 1% N2 (Gibco, Cat# 17502001), L-glutamine (final concentration 0.8 mM, Gibco, Cat# 25030081), Penicillin-Streptomycin (final concentration 100 U/mL, Corning, Cat# 30-002-CI), and 5 mM or 2 mM D-glucose.

Retinal organoids—An hiPSC line derived from CD34+ cord blood was used in this study (ThermoFisher Scientific, Cat# A18945[46]). This cell line was obtained with verified normal karyotype and contamination-free. Undifferentiated hiPSCs and derived retinal organoids were routinely tested for Mycoplasma contamination by PCR. The hiPSCs were enzymatically dissociated into small clumps and cultured in mTeSR1 medium and 10 mM Blebbistatin (Sigma, Cat# 1177356-70-5) to induce aggregate formation. Aggregates were gradually transitioned into neural-induction medium (NIM) on day 3. On day 7, aggregates were seeded onto Matrigel-coated dishes containing NIM at an approximate density of 20 aggregates per cm^2. On day 16, NIM were replaced with DMEM/F12 (3:1) supplemented with 2% B27 (without vitamin A, Invitrogen), 1x NEAA and 1% antibiotic– antimycotic (Gibco). Fourth week of differentiation, horseshoeshaped neural retina was manually detached with a sharpened Tungsten needle, collected and cultured in suspension at 37°C in a humidified 5% CO_2 incubator, where they gradually formed 3D retinal cups. To promote photoreceptor maturation, suspension cultures of retinal cups were supplemented

daily with 1 mM all-trans retinoic acid (Sigma, Cat# 302-79-4) at week 7–17.[47] Retinal organoids at 120 days of differentiation were used for experiments.

Hypoglycemia assay—To prepare media containing different concentrations of glucose, the D-glucose (Sigma, Cat# G5767) or L-glucose (Sigma, Cat# G5500) was added into DMEM (without D-glucose, Gibco, Cat# 11-966-025) for cell culture, or into Neurobasal-A Medium (without D-glucose, ThermoFisher, Cat# A2477501) for retinal explants. For cultured cells, after cell reached 90% confluence, the normal glucose DMEM media was changed with low glucose DMEM media for further culture. For retinal explants, the retinal explant was immediate incubated in Neurobasal-A Medium containing either 5 mM D-glucose or 2 mM D-glucose.

NAD/NADH assay—The retinal explants cultured in Neurobasal-A Medium (ThermoFisher, Cat# A2477501) containing 5 mM or 2 mM D-glucose were used for testing NAD/NADH with NAD/NADH Assay Kit (Colorimetric, Abcam, Cat# ab65348). One retinal explant was digested in 120 μL NADH/NAD Extraction Buffer. After centrifuge in 10 kD Spin Column (Abcam, Cat# ab93349 at 14,000 x g for 20 min at 4°C, half sample were transferred to a new tube and incubated at 60°C for 30 min to decompose NAD^+, while the remaining half was used as NADt (NADH plus NAD^+). 20 μL NADt and 20 μL decompose NAD^+ sample were mixed with 30 μL Extraction Buffer and then incubated with 100 μL of Reaction Mix at RT for 5 min to convert NAD^+ to NADH. After adding 10 μL of NADH Developer into each well and mix. Let the reaction cycle at room temperature for 20 min. The sample outputs were measured at OD 450 nm on a microplate reader in a kinetic mode.

L-lactate assay—L-Lactate products in retinal explants were measured with L- Lactate Assay Kit (Abcam, Cat# ab65331). After cultured in Neurobasal-A Medium (ThermoFisher, Cat# A2477501) containing 5 mM or 2 mM D-glucose for indicated time, the retinal explants were digested in 200 μL Lactate Assay Buffer and centrifuged at 14,000 rpm at 4°C for 10 min. 30 μL supernatant from each sample were mixed with 20 μL Lactate Assay Buffer and 50 μL Reaction Mix. After incubating at room temperature for 30 min, the sample outputs were measured at OD 450 nm on a microplate reader in a kinetic mode.

Immunofluorescence—For immunofluorescence performed on fixed primary murine Müller cells, the cells were incubated with primary antibodies at 4°C overnight. After washing with PBS for three times, the cells were labeled with secondary antibodies associated with DAPI. For immunofluorescence detection in retinal explants, after fixing with 4% PFA at 4°C overnight, the explants were washed with PBS for three times and transferred in 30% sucrose at 4°C overnight. The retinal explants were then immersed in OCT. 14 μm thick cryostat sections were generated for immunofluorescence. Sections were blocked in 5% BSA in PBST for 30 min at room temperature and incubated with the desired primary antibodies at 4°C overnight. The next day, the sections were washed with PBS for 3 × 10 min, followed by incubation with secondary antibodies for 1-2 h at room temperature. After additional 3 × 10 min washes with PBS, the slides were sealed with VECTASHIELDR

Antifade Mounting Media (Vector Laboratories, H-1200). Images were captured using a confocal microscope LSM 710 META (Carl Zeiss).

For immunofluorescence performed on human retinal organoids, samples were fixed in 4% paraformaldehyde for 1 h, washed twice in PBS, and cryoprotected with a sucrose gradient (6.75, 12.5, and 25%, overnight at 4°C) with a final incubation in 25% sucrose/OCT (2:1 ratio respectively) for 1 h at room temperature. Samples were embedded in 25% sucrose/OCT Tissue-Tek (Sakura), frozen, and stored at −80°C until used. Cryosections of 12- to 16-μm thickness were obtained and collected on Superfrost Plus slides. Sections were air-dried for 1 h, washed three times in PBS, blocked in 10% goat serum in PBS with 0.25% Triton X-100 for 1 h at room temperature, and incubated overnight with a primary antibody in 2% goat serum in PBS with 0.05% Triton X-100 at 4°C. The next day, the slides were washed three times in PBS and incubated with an Alexa Fluor–conjugated secondary antibody (1:500; Molecular Probes) in PBS for 1 h in the dark at room temperature. The slides were then washed three times in PBS, incubated in 4′,6-diamidino-2-phenylindole (1:1000 in PBS) for 10 min, and cover-slipped using DAKO fluorescent mounting medium. Fluorescence images were acquired with a Nikon C2 laser scanning confocal microscope (Melville, NY, USA). The images were minimally processed using Adobe Photoshop CS5 (San Diego, CA, USA).

All images are representative of at least three independent experiments. A list of antibodies used in this study is provided in key resources table. The dilution details were listed in Table S2.

Quantitative real-time RT-PCR—mRNA was isolated from cultured cells with RNeasy Mini Kit at indicated time points (Ambion, Cat# 12183025), and cDNA was prepared with MuLV Reverse Transcriptase (Qiagen, Cat# 205311). Quantitative real-time PCR was performed with Power SYBR Green PCR Master Mix (Applied Biosystems, Cat# 25742) and MyiQ Real-Time PCR Detection System (Bio-Rad). Cyclophilin A or β-actin were used for normalization of mouse or human cell lines, respectively. Primers are listed in Table S1.

Western blot—Cells in culture dishes were washed with PBS and lysed using RIPA buffer (Sigma, Cat# R0278) with 1% protease inhibitor cocktail (Sigma, Cat# P2714-1BTL). Cell lysates were then solubilized in LDS-sample buffer (ThermoFisher, Cat# NP0007) and incubated for 10 min at 70°C. To isolate the nuclear and cytoplasmic proteins, the nuclear extract kit (Active motif, Carlsbad, CA; Cat# 40010) was used for nuclear and cytoplasmic fractions, and manufacturer's protocol was followed to isolate fractions. Lysates were subjected to 4–12% gradient SDS/PAGE (ThermoFisher, Cat# NW04125BOX). After blocking the membranes with 5% milk (Bio-Rad, Cat# 1706404), the membranes were then incubated with primary antibody (see key resources table and Table S2) overnight at 4°C. After washing, the membranes were incubated with the following secondary antibodies, HRP-linked Goat Anti-rabbit IgG (Cell signaling, Cat# 7074, RRID:AB_2099233; 1:5,000), or HRP-linked Horse Anti-mouse IgG (Cell signaling, Cat# 7076, RRID:AB_330924; 1:5,000) for 1 h and then visualized with SuperSignal West Pico PLUS Chemiluminescent Substrate (ThermoFisher, Cat# 34580, 1: 4,000). Western blot scans are representative of at

least three independent experiments. A list of antibodies used in this study is provided in key resources table.

Blood glucose and media glucose measurement—A portable glucose meter (OneTouch UltraMini, LifeScan, Switzerland) was used to test both blood glucose and media glucose concentration. The measure range of the meter is 20–450 mg/dL (1.1–25 mM) glucose. For mice blood glucose measurement, blood from tail-tip were collected for measurement. For MIO-M1 cells, cells were incubated in DMEM containing 5mM glucose at 37° C in a CO_2 incubator until the cells are 70–80% confluent. Then media were changed with DMEM containing either 5 mM or 2 mM glucose and cells were incubated in normoxic or hypoxic conditions. Media glucose concentration was measured at indicated time points in Figure S3. For retinal explants, one retinal explant was placed onto one 30-mm diameter filter (Millipore, Cat# PICM03050) with the RGC side facing up, and the filter was placed into 6-well plate with 1.5 mL Neurobasal-A Medium (ThermoFisher, Cat# A2477501) prepared as described above. Media glucose concentration was measured at indicated time points in Figure S5.

Tubule formation—To prepare conditioned medium, MIO-M1 cells were cultured in DMEM containing normal (5 mM) glucose under 20% O_2, or in DMEM containing high (20 mM), normal (5 mM) or low (2 mM) glucose under 1% O_2 for 24 h. The conditioned media were collected for treatment of HMECs. Tubule formation assay was performed using growth factor-reduced Matrigel (BD Biosciences; Cat# 356231). 60 μL of Matrigel was added into a pre-chilled 96-well plate and placed in a 37°C CO_2 incubator for 30 min. 2×10^4 HMECs per well were then plated on the Matrigel in a 96-well plate. They were treated with conditioned medium for 18 h. Then images were captured and analyzed using ImageJ software. Total tube length was used to determine the tubule formation.

Directed *in vivo* angiogenesis assay—The Directed *in vivo* Angiogenesis Assay (DIVAA) was performed according to the manufacturer's protocol (Trevigen Inc., Gaithersburg, USA). In details, four sterile silicone cylinders-angioreactors (Trevigen, Gaithersburg, MD; Cat# 3450-048-01) filled with matrigel and conditioned media from MIO-M1 cells cultured in normal (5 mM) glucose under normoxia (20% O_2), or in high (20 mM), normal (5 mM), or low (2 mM) glucose under hypoxia (1% O_2) for 48 h. Then those angioreactors were subcutaneously implanted into the dorsal flank of each 8-week-old nu/nu mice (Charles River Laboratories, Vermont, USA). At day 14, the animals were euthanized by cervical dislocation and the angioreactors were collected and analyzed. Values for cell invasion are calculated by the ratio of relative fluorescent units (RFUs) of the test sample to control sample.

ELISA—ANGPTL4 (DuoSet, Cat# DY3485) and VEGF (Quantikine, Cat# MMV00) ELISA kits were purchased from R&D Systems. Conditioned media from MIO-M1 cells was diluted 1:1 in cell culture medium and analyzed for ANGPTL4 and VEGF with ELISAs performed according to the manufacturer's protocols.

Human phospho-kinase arrays for MIO-M1 cells—MIO-M1 cells were seeding on 15-mm diameter dish with 70–80% confluency. The second day, media was changed with

DMEM containing either 5 mM or 2 mM glucose. After incubation for 20 min, cells were harvest with 100 μL lysis buffer with 1% protease inhibitor cocktail (Sigma, Cat# P2714-1BTL), and proceeded for phosphorylation analysis according to the manufacture provided by Human Phosphor-Kinase Array Kit (R&D systems, Cat# ARY003C).

Insulin injection—To generate hypoglycemic condition *in vivo*, 8-10-week-old mice were intraperitoneally injected with insulin (4 U/kg body weight, Novolin N, NDC# 0169-1834-11). Blood glucose was measured 30 min after injection. Mice with blood glucose concentration of 40 mg/dL or lower were deemed hypoglycemic. Mice with blood glucose levels higher than 40 mg/dL will receive an additional dose of insulin (1 U/kg). The second and third dose of insulin (2U/kg) were intraperitoneally injected at 3 and 6 h after the first dose. The retina was isolated at 8 h after the first dose administration for the following experiments.

For insulin plus digoxin (Sigma, Cat# D6003) injection, 8-10-week-old mice were first intraperitoneally injected with digoxin (2 mg/kg body weight) to decrease HIF level. 2 h later, the mice were intraperitoneally injected with insulin (4 U/kg body weight, Novolin N, NDC# 0169-1834-11).

QUANTIFICATION AND STATISTICAL ANALYSIS

Results are shown as mean ± SD from at least three independent experiments. Statistical differences between groups were determined by Student's t-test with two-tailed hypothesis. GraphPad Prism 9 software was used for statistical analysis. $*p < 0.05$; $**p < 0.01$; $***p < 0.001$; $****p < 0.0001$; NS, non-significant.

Supplementary Material

Refer to Web version on PubMed Central for supplementary material.

ACKNOWLEDGMENTS

REFERENCES

1. Lam DW, and LeRoith D (2012). The worldwide diabetes epidemic. Curr. Opin. Endocrinol. Diabetes Obes 19, 93–96. 10.1097/MED.0b013e328350583a. [PubMed: 22262000]

2. Barrett EJ, Liu Z, Khamaisi M, King GL, Klein R, Klein BEK, Hughes TM, Craft S, Freedman BI, Bowden DW, et al. (2017). Diabetic microvascular disease: an endocrine society scientific statement. J. Clin. Endocrinol. Metab 102, 4343–4410. 10.1210/jc.2017-01922. [PubMed: 29126250]

3. Holman RR, Paul SK, Bethel MA, Matthews DR, and Neil HAW (2008). 10-year follow-up of intensive glucose control in type 2 diabetes. N. Engl. J. Med 359, 1577–1589. 10.1056/NEJMoa0806470. [PubMed: 18784090]

4. Holman RR, Paul SK, Bethel MA, Neil HAW, and Matthews DR (2008). Long-term follow-up after tight control of blood pressure in type 2 diabetes. N. Engl. J. Med 359, 1565–1576. 10.1056/NEJMoa0806359. [PubMed: 18784091]

5. Zoungas S, Arima H, Gerstein HC, Holman RR, Woodward M, Reaven P, Hayward RA, Craven T, Coleman RL, and Chalmers J; Collaborators on Trials of Lowering Glucose CONTROL group (2017). Effects of intensive glucose control on microvascular outcomes in patients with type 2 diabetes: a meta-analysis of individual participant data from randomised controlled trials. Lancet Diabetes Endocrinol. 5, 431–437. 10.1016/S2213-8587(17)30104-3. [PubMed: 28365411]

6. Bain SC, Klufas MA, Ho A, and Matthews DR (2019). Worsening of diabetic retinopathy with rapid improvement in systemic glucose control: a review. Diabetes Obes. Metab 21, 454–466. 10.1111/dom.13538. [PubMed: 30226298]

7. Antonetti DA, Klein R, and Gardner TW (2012). Diabetic retinopathy. N. Engl. J. Med 366, 1227–1239. 10.1056/NEJMra1005073. [PubMed: 22455417]

8. Early worsening of diabetic retinopathy in the diabetes control and complications trial. Arch. Ophthalmol 116, 874–886. 10.1001/archopht.116.7.874.

9. Frank RN (2004). Diabetic retinopathy. N. Engl. J. Med 350, 48–58. 10.1056/NEJMra021678. [PubMed: 14702427]

10. Gorst C, Kwok CS, Aslam S, Buchan I, Kontopantelis E, Myint PK, Heatlie G, Loke Y, Rutter MK, and Mamas MA (2015). Long-term glycemic variability and risk of adverse outcomes: a systematic review and meta-analysis. Diabetes Care 38, 2354–2369. 10.2337/dc15-1188. [PubMed: 26604281]

11. Suh S, and Kim JH (2015). Glycemic variability: how do we measure it and why is it important? Diabetes Metab. J 39, 273–282. 10.4093/dmj.2015.39.4.273. [PubMed: 26301188]

12. Hsu CR, Chen YT, and Sheu WHH (2015). Glycemic variability and diabetes retinopathy: a missing link. J. Diabetes Complicat 29, 302–306. 10.1016/j.jdiacomp.2014.11.013.

13. Awoniyi O, Rehman R, and Dagogo-Jack S (2013). Hypoglycemia in patients with type 1 diabetes: epidemiology, pathogenesis, and prevention. Curr. Diab. Rep 13, 669–678. 10.1007/s11892-013-0411-y. [PubMed: 23912765]

14. Liu S, Zhao Y, Hempe JM, Fonseca V, and Shi L (2012). Economic burden of hypoglycemia in patients with Type 2 diabetes. Expert Rev. Pharmacoecon. Outcomes Res 12, 47–51. 10.1586/erp.11.87. [PubMed: 22280196]

15. Snell-Bergeon JK, and Wadwa RP (2012). Hypoglycemia, diabetes, and cardiovascular disease. Diabetes Technol. Ther 14 (Suppl 1), S51–S58. 10.1089/dia.2012.0031. [PubMed: 22650225]

16. Domínguez RO, Pagano MA, Marschoff ER, González SE, Repetto MG, and Serra JA (2014). Alzheimer disease and cognitive impairment associated with diabetes mellitus type 2: associations and a hypothesis. Neurologia 29, 567–572. 10.1016/j.nrl.2013.05.006. [PubMed: 24140159]

17. Khan MI, Barlow RB, and Weinstock RS (2011). Acute hypoglycemia decreases central retinal function in the human eye. Vis. Res 51, 1623–1626. 10.1016/j.visres.2011.05.003. [PubMed: 21601590]

18. Cohen LH, and Noell WK (1960). Glucose catabolism of rabbit retina before and after development of visual function. J. Neurochem 5, 253–276. 10.1111/j.1471-4159.1960.tb13363.x. [PubMed: 13810977]

19. Winkler BS (1981). Glycolytic and oxidative metabolism in relation to retinal function. J. Gen. Physiol 77, 667–692. 10.1085/jgp.77.6.667. [PubMed: 6267165]

20. Kuwabara T, and Cogan DG (1961). Retinal glycogen. Arch. Ophthalmol 66, 680–688. 10.1001/archopht.1961.00960010682013. [PubMed: 14460992]

21. Winkler BS, Arnold MJ, Brassell MA, and Puro DG (2000). Energy metabolism in human retinal Muller cells. Invest. Ophthalmol. Vis. Sci 41, 3183–3190. [PubMed: 10967082]

22. Chen C, Pore N, Behrooz A, Ismail-Beigi F, and Maity A (2001). Regulation of glut1 mRNA by hypoxia-inducible factor-1. Interaction between H-ras and hypoxia. J. Biol. Chem 276, 9519–9525. 10.1074/jbc.M010144200. [PubMed: 11120745]

23. Yu AY, Shimoda LA, Iyer NV, Huso DL, Sun X, McWilliams R, Beaty T, Sham JS, Wiener CM, Sylvester JT, and Semenza GL (1999). Impaired physiological responses to chronic hypoxia in

mice partially deficient for hypoxia-inducible factor 1alpha. J. Clin. Invest 103, 691–696. 10.1172/JCI5912. [PubMed: 10074486]

24. Bosch-Marce M, Okuyama H, Wesley JB, Sarkar K, Kimura H, Liu YV, Zhang H, Strazza M, Rey S, Savino L, et al. (2007). Effects of aging and hypoxia-inducible factor-1 activity on angiogenic cell mobilization and recovery of perfusion after limb ischemia. Circ. Res 101, 1310–1318. 10.1161/CIRCRESAHA.107.153346. [PubMed: 17932327]

25. Otteson DC, and Phillips MJ (2010).A conditional immortalized mouse muller glial cell line expressing glial and retinal stem cell genes. Invest. Ophthalmol. Vis. Sci 51, 5991–6000. 10.1167/iovs.10-5395. [PubMed: 20505190]

26. Semenza GL (2007). Hypoxia-inducible factor 1 (HIF-1) pathway. Sci. STKE 2007, cm8. 10.1126/stke.4072007cm8. [PubMed: 17925579]

27. Zhang J, Qin Y, Martinez M, Flores-Bellver M, Rodrigues M, Dinabandhu A, Cao X, Deshpande M, Qin Y, Aparicio-Domingo S, et al. (2021). HIF-1alpha and HIF-2alpha redundantly promote retinal neovascularization in patients with ischemic retinal disease. J. Clin. Invest 131, e139202. 10.1172/JCI139202. [PubMed: 34128478]

28. Babapoor-Farrokhran S, Jee K, Puchner B, Hassan SJ, Xin X, Rodrigues M, Kashiwabuchi F, Ma T, Hu K, Deshpande M, et al. (2015). Angiopoietin-like 4 is a potent angiogenic factor and a novel therapeutic target for patients with proliferative diabetic retinopathy. Proc. Natl. Acad. Sci. USA 112, E3030–E3039. 10.1073/pnas.1423765112. [PubMed: 26039997]

29. Rodrigues M, Xin X, Jee K, Babapoor-Farrokhran S, Kashiwabuchi F, Ma T, Bhutto I, Hassan SJ, Daoud Y, Baranano D, et al. (2013). VEGF secreted by hypoxic Muller cells induces MMP-2 expression and activity in endothelial cells to promote retinal neovascularization in proliferative diabetic retinopathy. Diabetes 62, 3863–3873. 10.2337/db13-0014. [PubMed: 23884892]

30. Sodhi A, Ma T, Menon D, Deshpande M, Jee K, Dinabandhu A, Vancel J, Lu D, and Montaner S (2019). Angiopoietin-like 4 binds neuropilins and cooperates with VEGF to induce diabetic macular edema. J. Clin. Invest 129, 4593–4608. 10.1172/JCI120879. [PubMed: 31545295]

31. Sodhi A, and Montaner S (2015). Angiopoietin-like 4 as an emerging therapeutic target for diabetic eye disease. JAMA Ophthalmol. 133, 1375–1376. 10.1001/jamaophthalmol.2015.3723. [PubMed: 26469243]

32. Xin X, Rodrigues M, Umapathi M, Kashiwabuchi F, Ma T, Babapoor-Farrokhran S, Wang S, Hu J, Bhutto I, Welsbie DS, et al. (2013). Hypoxic retinal Muller cells promote vascular permeability by HIF-1-dependent up-regulation of angiopoietin-like 4. Proc. Natl. Acad. Sci. USA 110, E3425–E3434. 10.1073/pnas.1217091110. [PubMed: 23959876]

33. Jee K, Rodrigues M, Kashiwabuchi F, Applewhite BP, Han I, Lutty G, Goldberg MF, Semenza GL, Montaner S, and Sodhi A (2017). Expression of the angiogenic mediator, angiopoietin-like 4, in the eyes of patients with proliferative sickle retinopathy. PLoS One 12, e0183320. 10.1371/journal.pone.0183320. [PubMed: 28832635]

34. Rodrigues M, Kashiwabuchi F, Deshpande M, Jee K, Goldberg MF, Lutty G, Semenza GL, Montaner S, and Sodhi A (2016). Expression pattern of HIF-1alpha and VEGF supports circumferential application of scatter laser for proliferative sickle retinopathy. Invest. Ophthalmol. Vis. Sci 57, 6739–6746. 10.1167/iovs.16-19513. [PubMed: 27951596]

35. Feldser D, Agani F, Iyer NV, Pak B, Ferreira G, and Semenza GL (1999). Reciprocal positive regulation of hypoxia-inducible factor 1alpha and insulin-like growth factor 2. Cancer Res. 59, 3915–3918. [PubMed: 10463582]

36. Ryan HE, Poloni M, McNulty W, Elson D, Gassmann M, Arbeit JM, and Johnson RS (2000). Hypoxia-inducible factor-1alpha is a positive factor in solid tumor growth. Cancer Res. 60, 4010–4015. [PubMed: 10945599]

37. Semenza GL (2013). HIF-1 mediates metabolic responses to intratumoral hypoxia and oncogenic mutations. J. Clin. Invest 123, 3664–3671. 10.1172/JCI67230. [PubMed: 23999440]

38. Zhang H, Qian DZ, Tan YS, Lee K, Gao P, Ren YR, Rey S, Ham-mers H, Chang D, Pili R, et al. (2008). Digoxin and other cardiac glycosides inhibit HIF-1alpha synthesis and block tumor growth. Proc. Natl. Acad. Sci. USA 105, 19579–19586. 10.1073/pnas.0809763105. [PubMed: 19020076]

39. Paulus YM, and Sodhi A (2017). Anti-angiogenic therapy for retinal disease. Handb. Exp. Pharmacol 242, 271–307. 10.1007/164_2016_78. [PubMed: 27783271]

40. Wood JPM, Chidlow G, Graham M, and Osborne NN (2005). Energy substrate requirements for survival of rat retinal cells in culture: the importance of glucose and monocarboxylates. J. Neurochem 93, 686–697. 10.1111/j.1471-4159.2005.03059.x. [PubMed: 15836627]

41. Petit L, Ma S, Cipi J, Cheng SY, Zieger M, Hay N, and Punzo C (2018). Aerobic glycolysis is essential for normal rod function and controls secondary cone death in retinitis pigmentosa. Cell Rep. 23, 2629–2642. 10.1016/j.celrep.2018.04.111. [PubMed: 29847794]

42. Krispel C, Rodrigues M, Xin X, and Sodhi A (2013). Ranibizumab in diabetic macular edema. World J. Diabetes 4, 310–318. 10.4239/wjd.v4.i6.310. [PubMed: 24379922]

43. Miyata T, Suzuki N, and van Ypersele de Strihou C (2013). Diabetic nephropathy: are there new and potentially promising therapies targeting oxygen biology? Kidney Int. 84, 693–702. 10.1038/ki.2013.74. [PubMed: 23486514]

44. Catrina SB, and Zheng X (2016). Disturbed hypoxic responses as a pathogenic mechanism of diabetic foot ulcers. Diabetes. Metab. Res. Rev 32 (Suppl 1), 179–185. 10.1002/dmrr.2742. [PubMed: 26453314]

45. Johnson TV, and Martin KR (2008). Development and characterization of an adult retinal explant organotypic tissue culture system as an in vitro intraocular stem cell transplantation model. Invest. Ophthalmol. Vis. Sci 49, 3503–3512. 10.1167/iovs.07-1601. [PubMed: 18408186]

46. Burridge PW, Thompson S, Millrod MA, Weinberg S, Yuan X, Peters A, Mahairaki V, Koliatsos VE, Tung L, and Zambidis ET (2011). A universal system for highly efficient cardiac differentiation of human induced pluripotent stem cells that eliminates interline variability. PLoS One 6, e18293. 10.1371/journal.pone.0018293. [PubMed: 21494607]

47. Zhong X, Gutierrez C, Xue T, Hampton C, Vergara MN, Cao LH, Peters A, Park TS, Zambidis ET, Meyer JS, et al. (2014). Generation of three-dimensional retinal tissue with functional photoreceptors from human iPSCs. Nat. Commun 5, 4047. 10.1038/ncomms5047. [PubMed: 24915161]

Author Manuscript

Author Manuscript

Author Manuscript

Author Manuscript

Highlights

- Diabetic patients experience brief episodes of low glucose (hypoglycemia) each day

- In retinal glial cells, hypoglycemia promotes the HIF-dependent expression of GLUT1

- Hypoglycemia increases expression of HIF-dependent angiogenic mediators

- This physiologic response causes paradoxical worsening of diabetic retinopathy
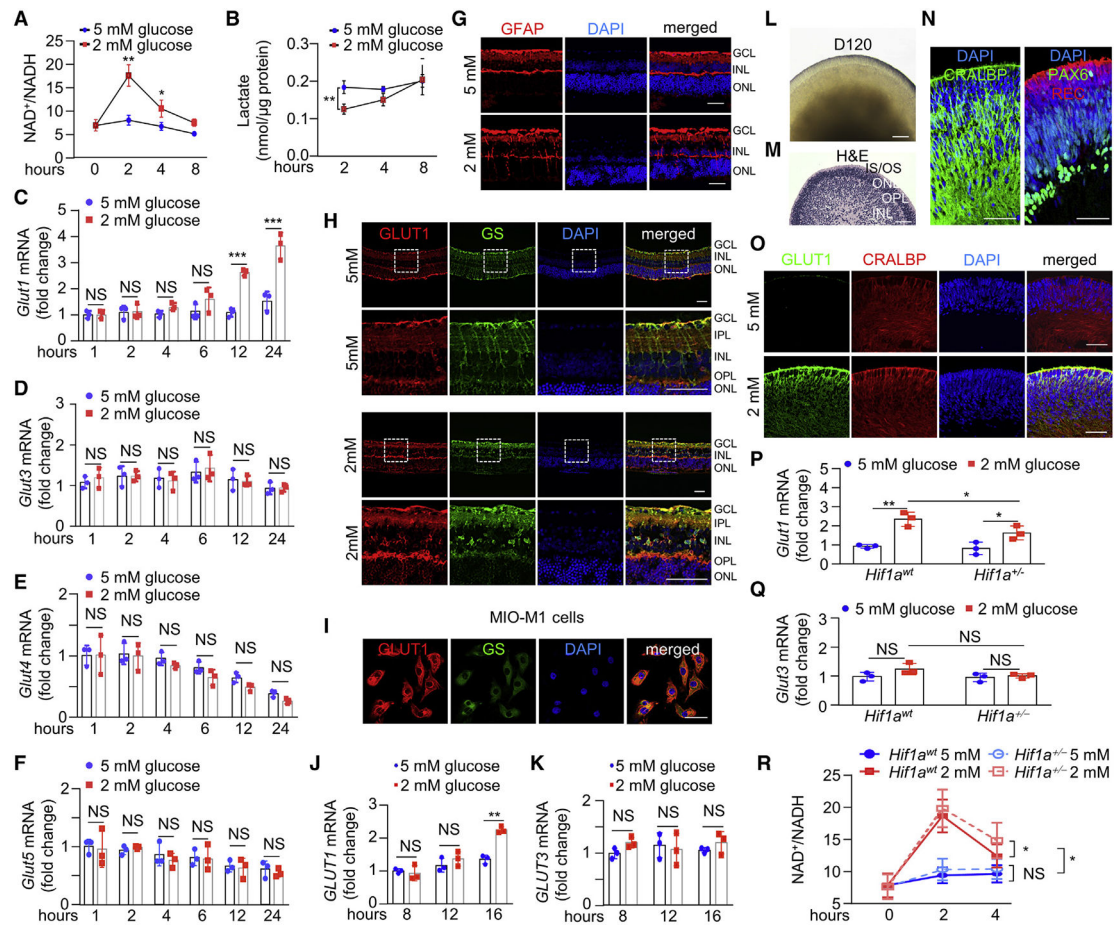
Figure 1. HIF-1-dependent aerobic glycolysis in retinal Müller glial cells cultured in low glucose

(A and B) NAD$^+$/NADH (A) and Lactate concentration (B) changes in retinal explants cultured in normal (5 mM) or low glucose (2 mM) for 0, 2, 4, and 8 h, respectively (n = 3 mice at each time point).

(C–F) *Glut1* (C), *Glut3* (D), *Glut4* (E), and *Glut5* (F) mRNA expression in retinal explants cultured in media containing 5 or 2 mM glucose under 20% O$_2$ over time. *Cyclophilin A* was used as an internal control.

(G) GFAP (red) expression in retinal explants after cultured in media containing 5 or 2 mM glucose for 24 h.

(H) GLUT1 (red) and GS (green) co-expression in Müller glial cells in retinal explants cultured in media containing 5 or 2 mM glucose for 24 h.

(I) GLUT1 expression in MIO-M1 cells.

(J and K) *Glut1* (J) and *Glut3* (K) mRNA expression in MIO-M1 cells cultured in media containing 5 or 2 mM glucose over time. *β-actin* was used as an internal control.

(L and M) Brightfield (L) and H&E staining (M) of D120 3D retinal organoids derived from hiPSCs.

(N) Immunofluorescence staining of Müller glial cells (expressing CRALBP, green) and outer retina photoreceptors (expressing recoverin, red), mitotic retinal progenitors within the neuroblastic layer (expressing low levels of Pax6, green), and amacrine cells (expressing high levels of Pax6, green).

(O) GLUT1 (green) and Müller glial cells marker CRALBP (red) expression in D120 3D retinal organoids cultured in 5 and 2 mM glucose and 20% O_2 for 4 h

(P and Q) *Glut1* (P) and *Glut3* (Q) mRNA levels in retinal explants from mice heterozygous for *Hif1a (Hif1a*$^{+/-}$*)* or their wild-type littermate controls (*Hif1a*^{wt}) cultured in media containing 5 or 2 mM glucose for 24 h.

(R) NAD$^+$/NADH in retinal explants from *Hif1a*$^{+/-}$ or *Hif1a*^{wt} cultured in media containing 5 or 2 mM glucose under 20% O_2 for 0, 2, and 4 h (n = 9 mice at each time point). GLUT1, glucose transporter 1; GFAP, glial fibrillary acidic protein; GS, glutamate synthetase; DAPI, diamidino-2-phenylindole; D120 = 120 days in culture; CRALBP, cellular retinaldehyde-binding protein; Rec, recoverin; Pax6, paired box 6; D-glu, D-glucose; GCL, ganglion cell layer; IPL, inner plexiform layer; INL, inner nuclear layer; OPL, outer plexiform layer; ONL, outer nuclear layer. IS/OS, inner segment/outer segment of photoreceptor. Scale bars, 50 μm. The values presented are the means ± SD of three independent experiments. *p < 0.05; **p < 0.01; ***p < 0.001; NS, non-significant. See also Figures S1 and S2.
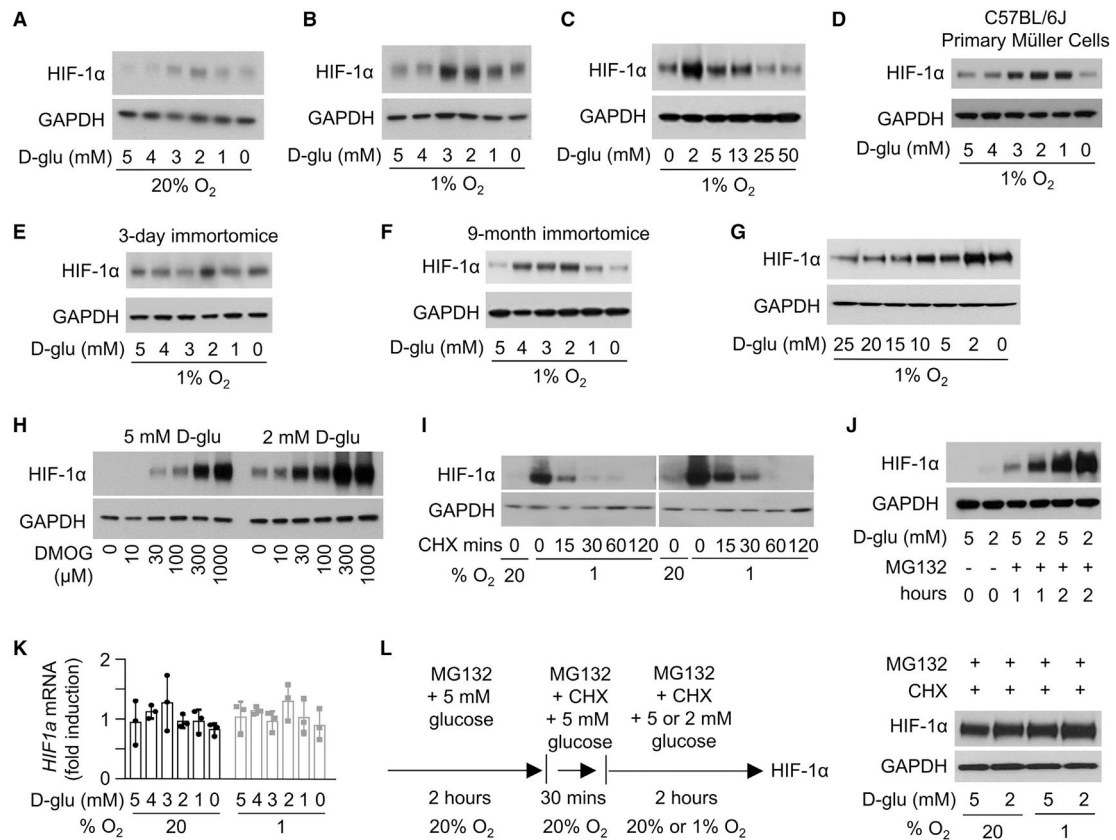
Figure 2. Enhanced translation of HIF-1α protein in MIO-M1 and primary mouse retinal Müller cells cultured in low glucose

(A and B) Western blot demonstrating expression of HIF-1α in MIO-M1 cells exposed to decreasing concentrations of glucose (5, 4, 3, 2, 1, or 0 mM) under 20% O_2

(A) and 1% O_2 (B) for 2 h.

(C) Immunoblot images for HIF-1α expression from MIO-M1 cells cultured in a wide range of glucose concentrations (0, 2, 5, 13, 25, or 50 mM) for 2 h.

(D) Western blot demonstrating HIF-1α expression in primary retinal Müller glial cells isolated from 3-day-old C57BL/6J mice and exposed to low glucose (5, 4, 3, 2, 1, or 0 mM) for 2 h.

(E and F) Immunoblot for HIF-1α expression in 3-day-old (E) and 9-month-old (F) immortomouse primary retinal Müller cells exposed to low glucose concentrations (5, 4, 3, 2, 1, or 0 mM) for 2 h.

(G) MIO-M1 cells were cultured in 25 mM glucose for 1 week (two serial passages). Culture medium was then changed to 25, 20, 15, 10, 5, 2, or 0 mM glucose for 2 h and immunoblot for HIF-1α.

(H) HIF-1α expression in MIO-M1 cells treated with the prolyl hydroxylase inhibitor DMOG (0, 10, 30, 100, 300, or 1,000 μM) in 5 or 2 mM glucose under 20% O_2 for 2 h.

(I) The half-life of HIF-1α was calculated by pre-treating MIO-M1 cells with 1% O_2 for 2 h, then exposing the cells to either 5 mM or 2 mM glucose in the presence of CHX (50 mg/mL) (for 15, 30, 60, or 120 min) under 1% O_2.

(J) HIF-1α expression in MIO-M1 cells treated with the proteasome inhibitor MG132 (5 μM) in 5 or 2 mM glucose in 20% O_2 for 1 or 2 h.

(K) *HIF1a* mRNA expression in MIO-M1 cells treated with 5, 4, 3, 2, 1, or 0 mM glucose under 20% or 1% O_2 for 24 h.

(L) Immunoblot of MIO-M1 cells pre-treated with MG132 for 2 h, followed by MG132 (5 μM) and CHX (50 μg/mL) for 30 min, and then exposed to 5 mM or 2 mM glucose for 2 h in 20% or 1% O_2. GAPDH antibody was used as loading control for all immunoblot experiments. The mRNA values presented are the means ± SD of three independent experiments. D-glu, D-glucose; MG132, proteasome inhibitor; CHX, cycloheximide. The values presented are the mean ± SD of three independent experiments. See also Figures S3 and S4.
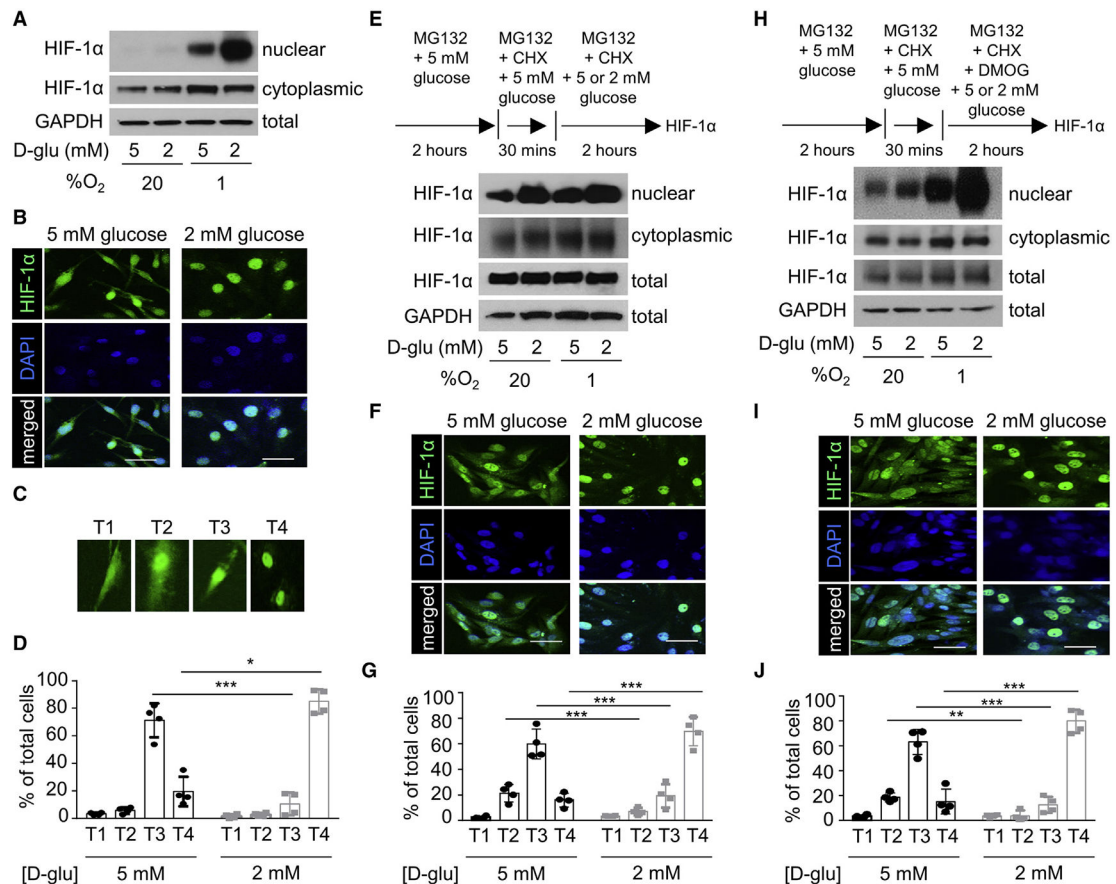
Figure 3. Enhanced nuclear localization of HIF-1α protein in Müller cells cultured in low glucose independent of HIF-1α protein translation

(A-D) MIO-M1 cells were treated with 5 or 2 mM glucose under 20% or 1% O_2 for 1 h. (A) Immunoblot for HIF-1α from nuclear and cytoplasmic fractions. (B) Representative images from immunofluorescence analysis of HIF-1α protein accumulation and nuclear localization in MIO-M1 cells under 1% O_2. (C) Subcellular localization of HIF-1α within cells was divided into four categories (T1–T4) depending on the presence of absence of HIF-1α proteins in the nucleus and/or cytoplasm. Type 1 (T1) = Equal (diffuse) HIF-1α localization in both the nucleus and the cytoplasm; Type 2 (T2) = HIF-1α localization in the nucleus greater than in the cytoplasm; Type 3 (T3) = HIF-1α localization predominantly in the nucleus, with scant cytoplasmic expression; and Type 4 (T4) = HIF-1α localization exclusively in the nucleus. (D) Quantification of HIF-1α localization in cells from (B) based on categories described in (C).

(E–G) MIO-M1 cells were pre-treated with MG132 for 2 h then with MG132 (5 μM) and CHX (50 μg/mL) together for 30 min. They were subsequently exposed to 5 or 2 mM glucose for 2 h under 20% or 1% O_2 in the presence of MG132 (5 μM) and CHX (50 μg/mL). (E) Immunoblot for HIF-1α from nuclear and cytoplasmic fractions. (F) Representative images from immunofluorescence analysis of HIF-1α protein accumulation and nuclear localization in MIO-M1 cells under 1% O_2. (G) Quantification of cells from (F). (H–J) MIO-M1 cells were pre-treated with MG132 (5 μM) for 2 h, then with MG132 (5 μM) and CHX (50 μg/mL) together for 30 min. They were subsequently exposed to 5 or

2 mM glucose for 2 h under 20% or 1% O_2 in the presence of MG132 (5 μM), CHX (50 μg/mL), and DMOG (100 μM). (H) Immunoblot for HIF-1α from nuclear and cytoplasmic fractions. (I) Representative images from immunofluorescence analysis of HIF-1α protein accumulation and nuclear localization in MIO-M1 cells under 1% O_2. (J) Quantification of cells from (I). The values presented are the means ± SD of three independent experiments. *$p < 0.05$; **$p < 0.01$; ***$p < 0.001$. D-glu, D-glucose; total, total cellular fraction; MG132, proteasome inhibitor; CHX, cycloheximide; DMOG, dimethyloxalylglycine. Scale bars, 50 μm.
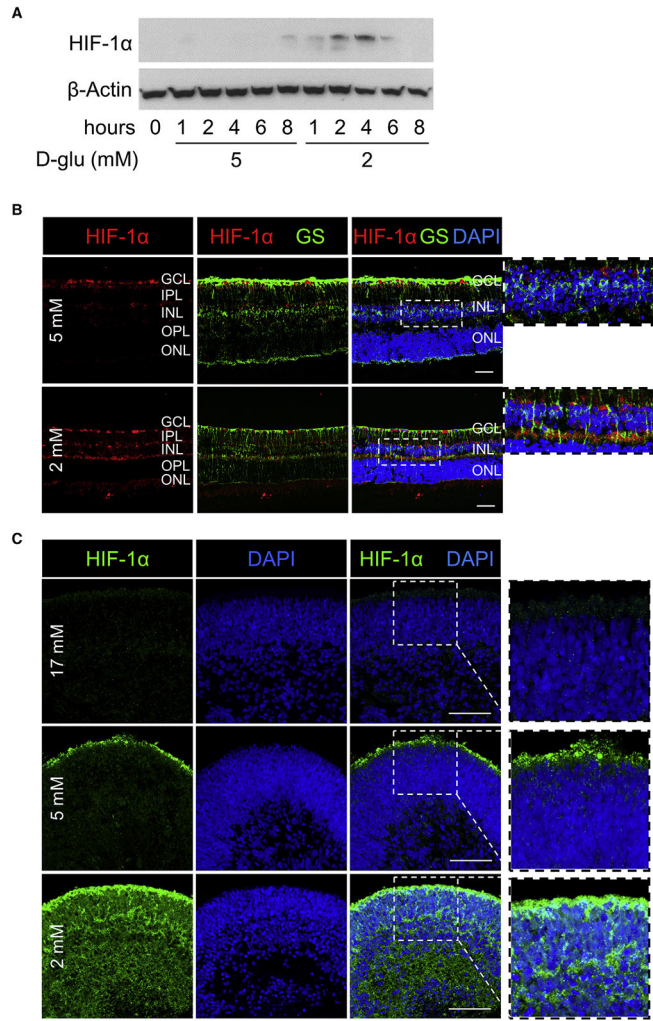
Figure 4. Increased HIF-1α protein accumulation in mouse retinal explants and human retinal organoids cultured in low glucose

(A) Immunoblot images for HIF-1α expression from mouse retinal explants cultured in media containing either 5 or 2 mM glucose under 20% O_2 for 1, 2, 4, 6, and 8 h.

(B) Representative immunohistochemistry images indicating HIF-1α (red) and GS (green) staining in the retina of mice treated with 5 mM glucose (upper panel) or 2 mM glucose (lower panel) under 20% O_2 for 4 h.

(C) HIF-1α expression in D120 3D retinal organoids cultured in 17 mM glucose (standard culture conditions for retinal organoids), 5 mM glucose, and 2 mM glucose and 20% O_2 for 4 h. GS, glutamate synthetase; DAPI, diamidino-2-phenylindole; GCL, ganglion cell layer; IPL, inner plexiform layer; INL, inner nuclear layer; OPL, outer plexiform layer; ONL, outer nuclear layer; Scale bar, 50 μm. See also Figure S5.
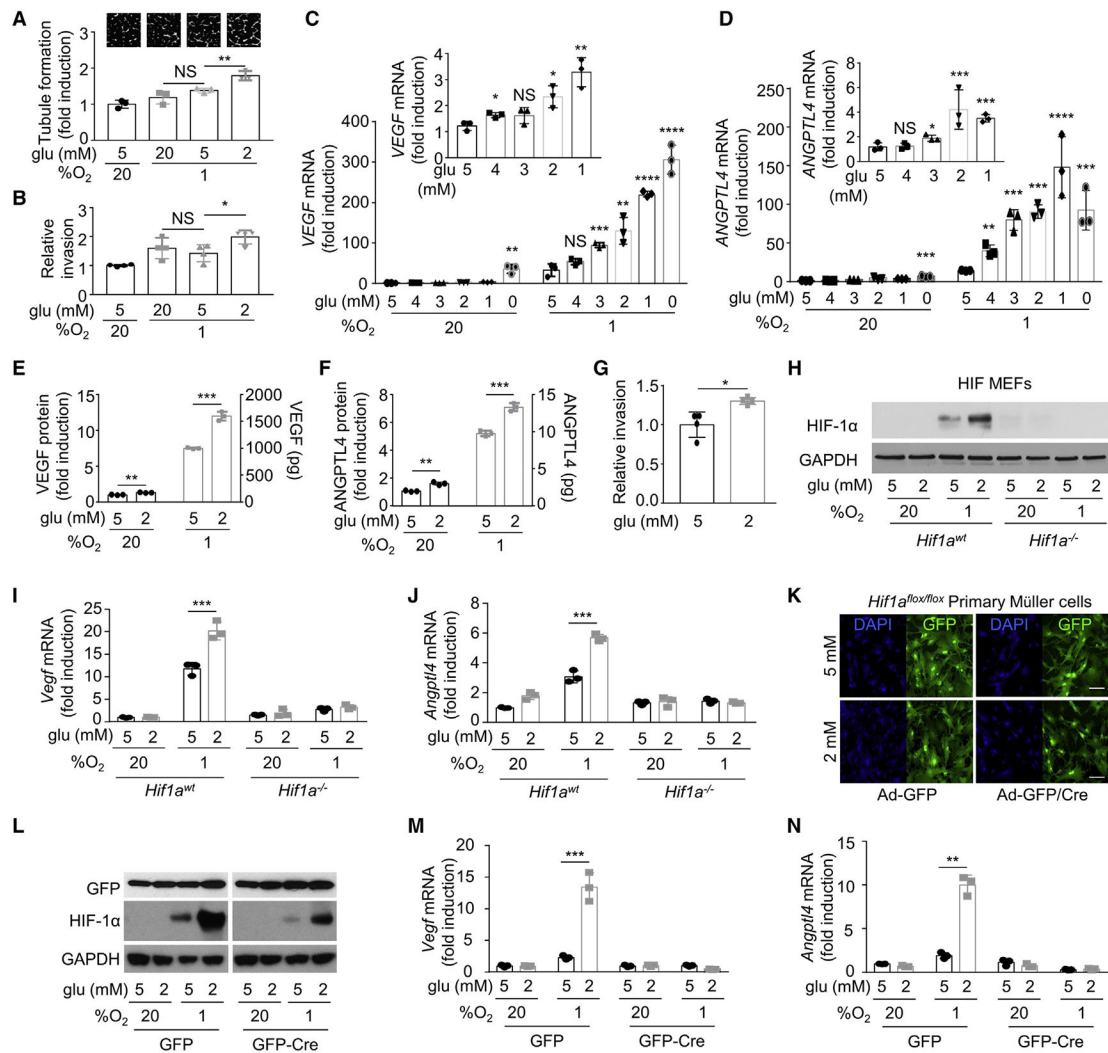
Figure 5. Retinal Müller glial cells cultured in low glucose demonstrate enhanced transcription of HIF-regulated angiogenic mediators

(A) Tubule formation by human microvascular endothelial cells (HMECs) treated with conditioned media from MIO-M1 cells exposed to 20, 5, or 2 mM glucose for 24 h, under serum starvation (1% serum) and exposed to normoxia (20% O_2) or hypoxia (1% O_2). Representative images of Matrigel-induced tubules (top) and quantification of the average number of tubules (bottom). For each condition, four random fields were digitally imaged and analyzed from three independent experiments each.

(B) Quantification of relative invasion from the directed *in vivo* angiogenesis assay (DIVAA) induced by the conditioned medium from MIO-M1 cells exposed to 20, 5, or 2 mM glucose for 24 h under serum starvation and exposed to 20% or 1% O_2.

(C and D) *VEGF* (C) and *ANGPTL4* (D) mRNA expression in MIO-M1 cells treated with 5, 4, 3, 2, 1, or 0 mM glucose under 20% or 1% O_2 for 24 h. Insert: mRNA expression of *VEGF* or *ANGPTL4* in cells cultured under different glucose concentrations under 20% O_2.

(E and F) VEGF (E) and ANGPTL4 (F) protein secretion in MIO-M1 cells treated with 5 or 2 mM glucose under 20% or 1% O_2 for 24 h.

(G) Media conditioned by MIO-M1 cells cultured under 20% O_2 and exposed to 2 mM glucose was used in the DIVAA assay to check for its angiogenic potential compared with conditioned media from MIO-M1 cells exposed to 5 mM glucose under 20% O_2.

(H–J) Mouse embryonic fibroblasts (MEFs) from wild-type (*Hif1a*[wt]) or *Hif1a*^{−/−} mice were treated with 5 or 2 mM glucose and exposed to 20% or 1% O_2.

(H) Protein from lysates collected after a 2-h treatment was used for immunoblotting.

(I and J) *Vegf* (I) and *Angptl4* (J) mRNA expression was determined after a 24-h treatment. *Cyclophilin A* was used as internal control.

(K) Primary Müller cells isolated from *Hif1a*[flox/flox] mice were infected with Ad5-CMV-Cre-eGFP to reduce HIF levels and cells were treated with 5 or 2 mM glucose.

(L) Immunoblot probed for GFP and HIF-1α after a 2-h treatment. Infection with Ad5-CMV-eGFP was used as a control.

(M and N) *Vegf* (M) and *Angptl4* (N) mRNA levels were determined after a 24-h treatment. The values presented are the means ± SD of three independent experiments. $^*p < 0.05$; $^{**}p < 0.01$; $^{***}p < 0.001$; $^{****}p < 0.0001$; NS, non-significant. glu, D-glucose. Scale bar, 50 μm.
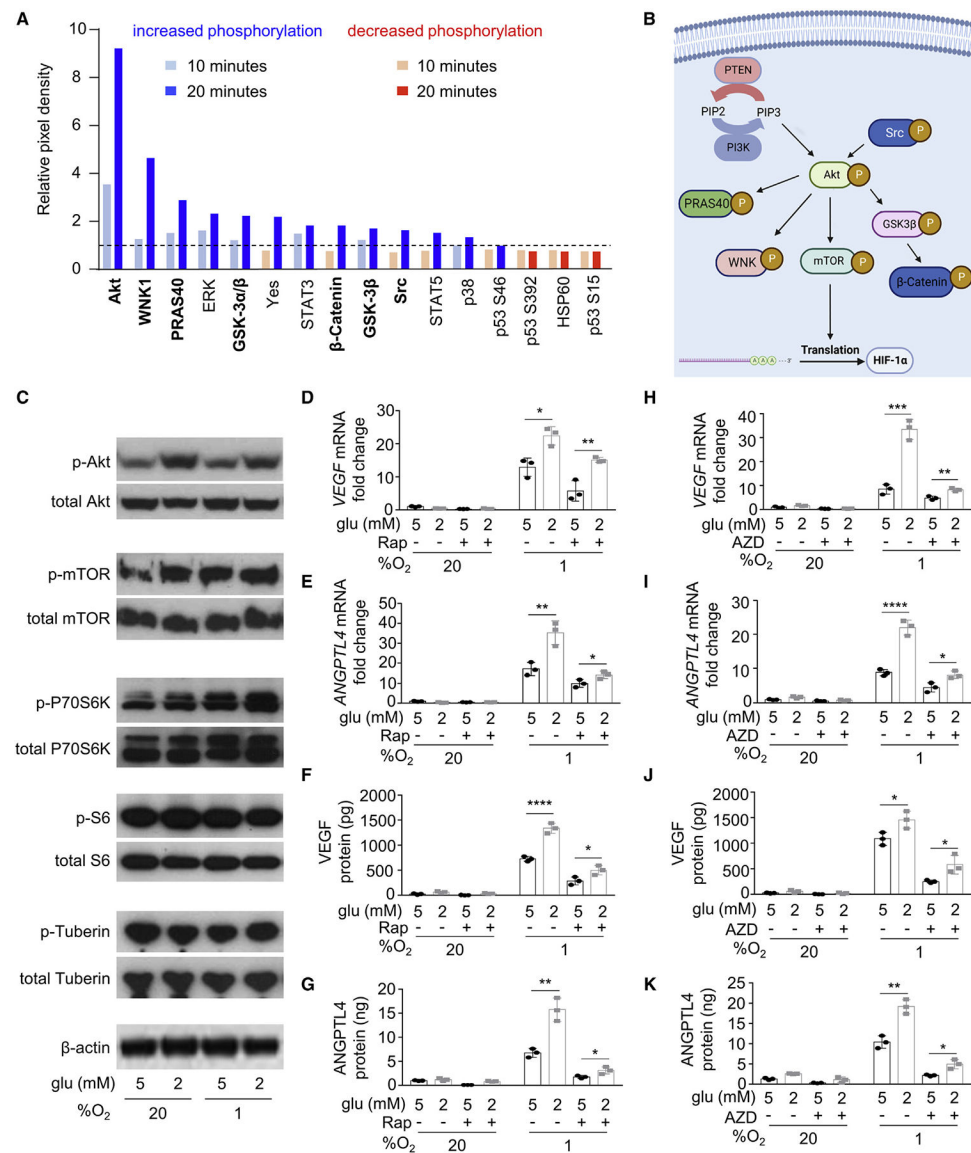
Figure 6. Activation of the Akt/mTOR pathway is not necessary for the promotion of HIF-1α accumulation in Müller glial cells cultured in low glucose

(A) Relative pixel density of phosphorylated kinases from MIO-M1 cells cultured in 2 mM glucose to 5 mM glucose for 10 min and 20 min. Bold font indicates kinases regulated by the Akt signaling pathway.

(B) Schematic depicting the regulation of HIF-1α translation by Akt/mTOR signaling pathway (BioRender).

(C) Representative immunoblots of protein extracts from MIO-M1 cells treated with 5 or 2 mM glucose under 20% O_2 or 1% O_2, and probed for p-Akt, t-Akt, p-mTOR, t-mTOR, p-P70S6K, t-P70S6K, p-S6, t-S6, p-Tuberin, or t-Tuberin. β-actin was used as a loading control.

(D–K) *VEGF* mRNA (D and H), *ANGPTL4* mRNA (E and I), VEGF protein (F and J), and ANGPLT4 (G and K) protein levels were tested after MIO-M1 cells were treated with 5 or 2 mM glucose under 1% O_2 in the presence of 1 mM Rapamycin (D–G) or AZD8055 (1 μM;

H–K). p, phospho, glu, D-glucose, Rap, rapamycin, AZD, AZD8055. β-actin was used as an internal control. The values presented are the mean ± SD of three independent experiments. $*p < 0.05$; $**p < 0.01$; $***p < 0.001$; $****p < 0.0001$; NS, non-significant. See also Figure S6.
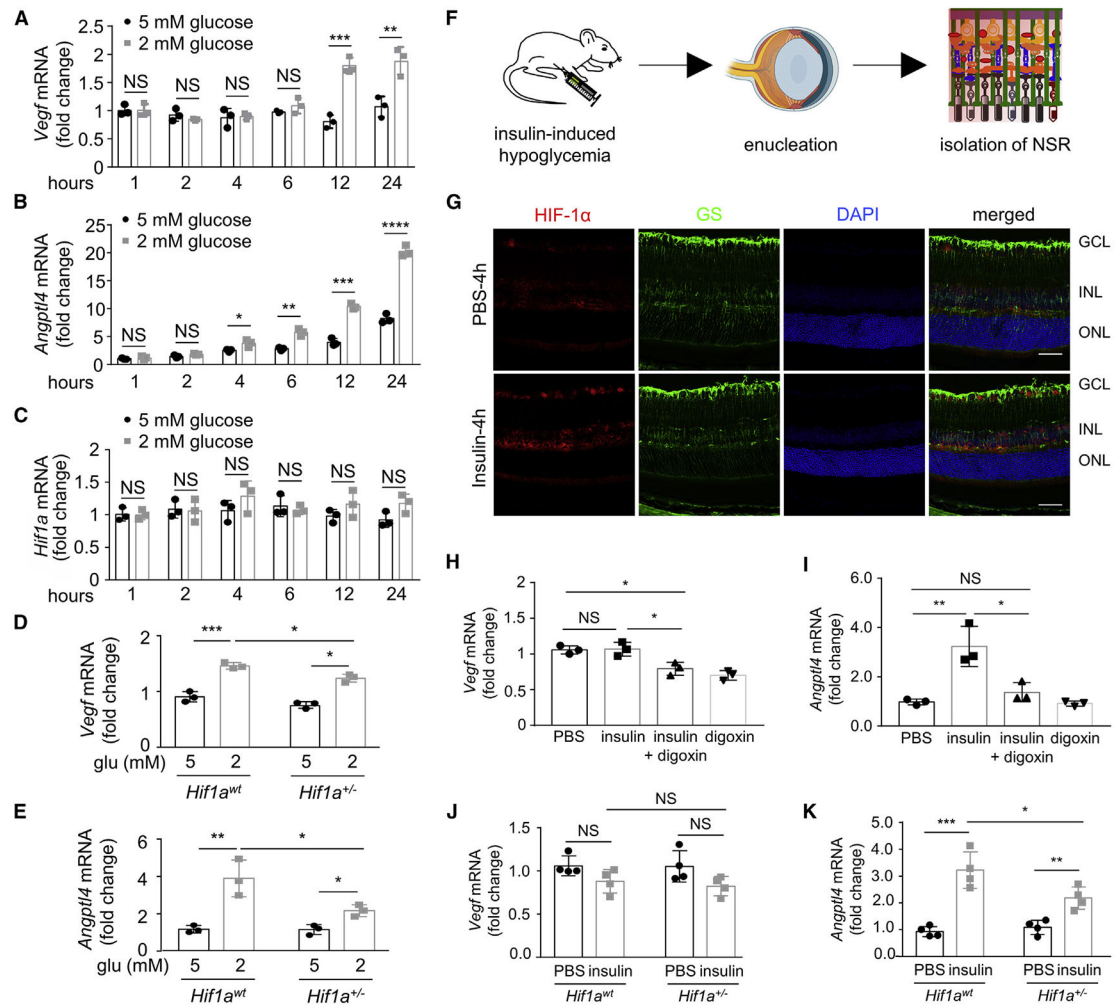
Figure 7. HIF-dependent increase in the expression of angiogenic mediators in mouse retina exposed to hypoglycemia

(A–C) *Vegf* (A), *Angptl4* (B), and *Hif1a* (C) mRNA expression was determined in retinal explants cultured in media containing 5 or 2 mM glucose over time.

(D and E) *Vegf* (D) and *Angptl4* (E) mRNA expression was determined in retinal explants from mice heterozygous for *Hif1a (Hif1a$^{+/-}$)* or their wild-type littermate controls (*Hif1a^{wt}*) cultured in media containing 5 or 2 mM glucose for 24 h.

(F) Schematic depicting steps for isolation of mRNA from neurosensory retina (NSR) of mice after injection with insulin. (G) Representative immunohistochemistry images indicating HIF-1α (red) and GS (green) staining in the retina of mice injected with PBS (upper panel) or insulin (bottom panel) for 4 h.

(H and I) *Vegf* (H) and *Angptl4* (I) mRNA expression was determined in retina from C57BL/6J mice injected with PBS, insulin, digoxin, or insulin plus digoxin for 8 h.

(J and K) *Vegf* (J) and *Angptl4* (K) mRNA expression was determined in retina from *Hif1a$^{+/-}$* and *Hif1a^{wt}* siblings injected with PBS or insulin for 8 h; n = 3–4 mice for each experiment. The values presented are the means ± SD of three independent experiments. *Cyclophilin A* was used as internal control. The values presented are the means ± SD of three independent experiments. *p < 0.05; **p < 0.01; ***p < 0.001; ****p < 0.0001; NS,

non-significant. GS, glutamate synthetase; DAPI, diamidino-2-phenylindole; GCL, ganglion cell layer; INL, inner nuclear layer; ONL, outer nuclear layer. Scale bars, 50 μm.

KEY RESOURCES TABLE

REAGENT or RESOURCE	SOURCE	IDENTIFIER
Antibodies		
Rabbit polyclonal anti-HIF-1a	Gene Tex	Cat# GTX127309; RRID:AB_2616089
Rabbit monoclonal anti-PHD2	Cell Signaling	Cat# 4835; RRID: N/A
Mouse monoclonal anti-GAPDH	Sigma	Cat# G8795; RRID:AB_1078991
Rabbit monoclonal anti-VHL	Cell Signaling	Cat# Cat# 2738; RRID:AB_2218190
Mouse monoclonal anti- Glutamine Synthetase (GS)	Millipore	Cat# MAB302; RRID:AB_2110656
Rabbit polyclonal anti-RBPMS	phosphosolutions	Cat# 1830-RBPMS; RRID:AB_2492225
Rabbit polyclonal anti-ISL1	Abcam	Cat# ab20670; RRID:AB_881306
Rabbit polyclonal anti-Glut1	Millipore	Cat# 07-1401; RRID:AB_11212210
Mouse monoclonal anti-NeuN	Millipore	Cat# MAB377; RRID:AB_2298772
Rabbit polyclonal anti-GFAP	Agilent DAKO	Cat# GA524; RRID:AB_2811722
Rabbit polyclonal anti-Vimentin	Abcam	Cat# ab45939; RRID:AB_2257290
Mouse monoclonal anti-PAX-6	DSHB	Cat# AB528427; RRID:AB_528427
Rabbit polyclonal anti- REC	Millipore	Cat# AB5585; RRID:AB_2253622
Mouse monoclonal anti- CRALBP	Abcam	Cat# ab15051; RRID:AB_2269474
Rabbit polyclonal anti-HIF-1a	Thermo Fisher	Cat# PA1-16601; RRID:AB_2117128
Rabbit monoclonal anti-GFP	Cell Signaling	Cat# 2956; RRID:AB_1196615
Rabbit polyclonal anti-b-actin	Cell Signaling	Cat# 4967; RRID:AB_330288
Rabbit monoclonal anti-p-AKT	Cell Signaling	Cat# 4060; RRID:AB_2315049
Rabbit monoclonal anti-t-AKT	Cell Signaling	Cat# 4691; RRID:AB_915783
Rabbit monoclonal anti-p-mTOR	Cell Signaling	Cat# 5536; RRID:AB_10691552
Rabbit monoclonal anti-t-mTOR	Cell Signaling	Cat# 2983; RRID:AB_2105622
Rabbit monoclonal anti-p-P70S6	Cell Signaling	Cat# 9206; RRID:AB_2285392
Rabbit monoclonal anti-t-P70S6	Cell Signaling	Cat# 9202; RRID:AB_331676
Rabbit monoclonal anti-p-S6	Cell Signaling	Cat# 4858; RRID:AB_916156
Rabbit monoclonal anti-t-S6	Cell Signaling	Cat# 2217; RRID:AB_331355
Rabbit monoclonal anti-p-Tuberin	Cell Signaling	Cat# 5584; RRID:AB_10698883
Rabbit monoclonal anti-t-Tuberin	Cell Signaling	Cat# 4308; RRID:AB_10547134
HRP-linked Goat Anti-rabbit IgG	Cell signaling	Cat# 7074; RRID:AB_2099233
HRP-linked Horse Anti-mouse IgG	Cell signaling	Cat# 7076; RRID:AB_330924
Alexa Fluor® 647 AffiniPure Donkey Anti-Mouse IgG	Jackson ImmunoResearch Labs	Cat# 715-605-150; RRID:AB_2340862
Alexa Fluor 647-AffiniPure Goat Anti-Mouse IgG	Jackson ImmunoResearch Labs	Cat# 115-605-006; RRID:AB_2338903
Fluorescein (FITC)-Donkey Anti-Rabbit IgG	Jackson ImmunoResearch Labs	Cat# 711-097-003; RRID:AB_2340598
Fluorescein (FITC)-AffiniPure Donkey Anti Mouse IgG	Jackson ImmunoResearch Labs	Cat# 715-095-150; RRID:AB_2340792
Rhodamine Red-X-AffiniPure Donkey Anti-Rat IgG	Jackson ImmunoResearch Labs	Cat# 712-295-150; RRID:AB_2340675
Rhodamine Red-X-AffiniPure F(ab')2 Fragment Donkey Anti-Rabbit IgG	Jackson ImmunoResearch Labs	Cat# 711-296-152; RRID:AB_2340614
Rhodamine Red-X-AffiniPure Donkey Anti-Mouse IgG	Jackson ImmunoResearch Labs	Cat# 715-295-150; RRID:AB_2340831
Bacterial and virus strains		
Ad5-CMV-eGFP	Adenovirus Vectors Service	N/A

REAGENT or RESOURCE	SOURCE	IDENTIFIER
Ad5-CMV-Cre-eGFP	Adenovirus Vectors Service	N/A
Chemicals, peptides, and recombinant proteins		
MG132	Sigma	Cat# M7449
Dimethyloxalylglycine (DMOG)	Cayman Pharmaceuticals	Cat# 71210
Cycloheximide	Cell Signaling	Cat# 2112
Digoxin	Sigma	Cat# D6003
Cycloheximide	Cell Signaling	Cat# 2112
Insulin	Novolin N	NDC# 0169-1834-11
D-glucose	Sigma	Cat# G5767
L-glucose	Sigma	Cat# G5500
Rapamycin	Selleck Chemicals	Cat# S1039
AZD8055	Selleck Chemicals	Cat# S1555
Critical commercial assays		
Tubule formation assay	BD Biosciences	Cat# 356231
Directed *in vivo* Angiogenesis Assay (DIVAA)	Trevigen Inc	Cat# 3450-048-01
Mouse ANGPTL4 ELISA Kit	DuoSet	Cat# DY3485
Mouse VEGF ELISA Kit	Quantikine	Cat# MMV00
NAD/NADH Assay Kit (Colorimetric)	Abcam	Cat# ab65348
L- Lactate Assay kit (Colorimetric)	Abcam	Cat# ab65331
human phosphor-Kinase Array Kit	R&D systems	Cat# ARY003C
Deposited data		
Raw and analyzed data	This paper	https://doi.org/10.17632/cx4zpmmwbx.1
Experimental models: Cell lines		
MIO-M1 cells	Astrid Limb lab	N/A
HMEC1	CDC	N/A
Hif1α $^{+/+}$ and Hif1α $^{-/-}$ MEFs	Gregg L. Semenza lab	N/A
hiPSC line	ThermoFisher Scientific	Cat# A18945
Experimental models: Organisms/strains		
Mice: C57BL/6J	Jackson laboratory	Stock No, 000,664
Mice: immortomouse	Jackson laboratory	Stock No, 032,619
Mice: nu/nu mice	Charles River Laboratories	Strain Code, 088
Mice: *Hif1a$^{flox/flox}$* mice	Jackson laboratory	Stock No, 007,561
Mice: *Hif1a$^{+/-}$*	Jackson laboratory	Stock No: 026,270
Oligonucleotides		
Primer sequences are listed in Table S1	This paper	N/A
Scrambled siRNA	Santa Cruz	Cat# sc-37007
HIF-1α siRNA	Santa Cruz	Cat# sc-35561
Recombinant DNA		
Plasmid: pCEFL-EGFP	Atsuko Sakurai et al., 2010	N/A
Plasmid: pCEFL-Full Length HIF-1α	gift from J. Silvio Gutkind	N/A
Software and algorithms		

REAGENT or RESOURCE	SOURCE	IDENTIFIER
ImageJ	NIH ImageJ	https://imagej.nih.gov/ij/
BioRender	BioRender	https://biorender.com/
Graph Pad Prism version 9	GraphPad Software	https://www.graphpad.com